3
Combustion Principles

3.1
Basic Combustion Calculations

3.1.1
Determination of the Quantity of Normal and Oxygenated Air Necessary for Complete Combustion

3.1.1.1 Air Requirement of Gaseous Fuels

In order to determine the oxygen and air required for complete combustion, one must use the elementary combustion reactions of the combustible components of the fuel gas, as listed in Table 3.1 and shown in Figure 3.1.

For example, if the fuel contains 85% CH_4, 10% H_2 and 5% N_2, then only the stoichiometric reactions of methane and hydrogen should be taken into consideration:

$$CH_4 + 2O_2 \rightarrow CO_2 + 2H_2O \tag{3.1}$$

$$H_2 + 0.5O_2 \rightarrow H_2O \tag{3.2}$$

The combustion of 1 mole of CH_4 requires 2 mole of O_2, while 1 mole H_2 requires 0.5 mole of O_2.

It is well known that the molar volume of any ideal gas is the same: 22.41 dm^3 mol^{-1} or 22.41 m^3 $kmol^{-1}$ at temperature 273.15 K and pressure101.3 kPa.

Thus the complete combustion of 22.4 m^3 CH_4 requires 44.8 m^3 O_2, while the complete combustion of 22.4 m^3 H_2 requires 11.2 m^3 O_2.

In the example above, 1 m^3 gaseous fuel contains 0.85 m^3 CH_4 and 0.1 m^3 H_2, thus the total oxygen needed for the complete combustion of the mixture is

$$V_{O_2} = (0.85 \cdot 2) + (0.1 \cdot 0.5) = 1.75\ m^3$$

If the combustion is supplied by dry air, then its normal composition can be used and 21% oxygen and 79% nitrogen can be assumed. In this case the nitrogen content of the air is $79/21 = 3.762$ times the volume of the stoichiometric oxygen. Alternatively, one can say, that the air required for a complete combustion is $100/21 = 4.76$ times the oxygen required.

Combustion: From Basics to Applications, First Edition. Maximilian Lackner, Árpád B. Palotás, and Franz Winter.

Table 3.1 Reactions and the products derived from the combustion of gaseous fuel components in the case of complete combustion at air factor $n = 1$, temperature 273.15 K and pressure 101.3 kPa.

Combustible Gas	Combustion Reaction	Oxygen $m^3\,m^{-3}$	Air Req. $m^3\,m^{-3}$	Flue gas Components $m^3\,m^{-3}$			Flue Gas Volume $m^3\,m^{-3}$	
		V_{O_2}	V_{air}	V_{CO_2}	V_{H_2O}	V_{N_2}	$V_{flue,\ wet}$	$V_{flue,\ dry}$
Carbon monoxide	$CO + 0.5\ O_2 = CO_2$	0.5	2.38	1	–	1.88	2.88	2.88
Hydrogen	$H_2 + 0.5\ O_2 = H_2O$	0.5	2.38	–	1	1.88	2.88	–
Methane	$CH_4 + 2O_2 = CO_2 + 2H_2O$	2.0	9.52	1	2	7.52	10.52	8.52
Ethane	$C_2H_6 + 3.5\ O_2 = 2CO_2 + 3H_2O$	3.5	16.65	2	3	13.15	18.15	15.15
Propane	$C_3H_8 + 5O_2 = 3CO_2 + 4H_2O$	5.0	23.80	3	4	18.80	25.80	21.80
Butane	$C_4H_{10} + 6.5\ O_2 = 4CO_2 + 5H_2O$	6.5	30.95	4	5	24.45	33.45	28.45
Pentane	$C_5H_{12} + 8O_2 = 5CO_2 + 6H_2O$	8.0	38.10	5	6	30.08	41.08	35.08
Hexane	$C_6H_{14} + 9.5\ O_2 = 6CO_2 + 7H_2O$	9.5	45.20	6	7	35.70	48.70	41.70
Heptane	$C_7H_{16} + 11\ O_2 = 7CO_2 + 8H_2O$	11.0	52.40	7	8	41.35	56.35	48.35
Octane	$C_8H_{18} + 12.5\ O_2 = 8CO_2 + 9H_2O$	12.5	59.50	8	9	47.00	64.00	55.00
Acetylene	$C_2H_2 + 2.5\ O_2 = 2CO_2 + H_2O$	2.5	11.90	2	1	9.40	12.40	11.40
Ethylene	$C_2H_4 + 3O_2 = 2CO_2 + 2H_2O$	3.0	14.30	2	2	11.28	15.28	13.28
Benzene	$C_6H_6 + 7.5\ O_2 = 6CO_2 + 3H_2O$	7.5	35.70	6	3	28.20	37.20	34.20

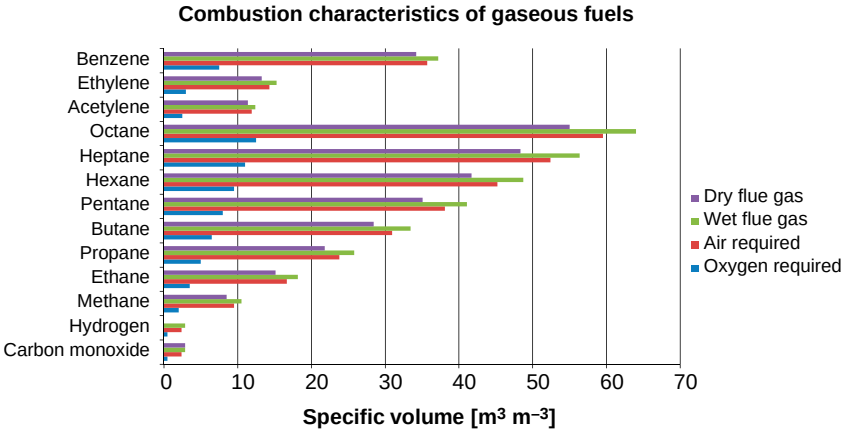

Figure 3.1 Combustion characteristics of the most common gaseous fuels at stoichiometric ratios and complete combustion: oxygen and air required, wet and dry flue gas produced per unit volume of the fuel gas.

Consequently, in the example above the air requirement for $1\,m^3$ fuel is the following:

$$V_{air} = 1.75 + (1.7 \cdot 3.76) = 8.34\,m^3$$

or

$$V_{air} = 1.75 \cdot 4.76 = 8.34\,m^3$$

The general equation of the theoretical (stoichiometric) air requirement of the perfect combustion of a gaseous fuel mixture is – based on the stoichiometric reactions of all combustible components as shown in Table 3.1 – the following:

$$V_{air,stoich} = 0.0476\,(0.5 \cdot CO + 0.5 \cdot H_2 + 2 \cdot CH_4 + 3.5 \cdot C_2H_6 + 5 \cdot C_3H_8 + \ldots + 2.5 \cdot C_2H_2 + \quad +3 \cdot C_2H_4 + 7.5 \cdot C_6H_6 - O_2), m^3m^{-3} \tag{3.3}$$

In reality – due to imperfect mixing in practical cases –more air than the stoichiometric amount is needed, which is calculated as follows:

$$V_{air} = \lambda \cdot V_{air,stoich}\ m^3m^{-3} \tag{3.4}$$

In Eq. (3.4), λ is the air factor (also called excess air factor), the ratio of the actual air supply to the stoichiometric one. Its value is dependent on the mixing efficiency of the fuel and the combustion air. Typical values for gaseous fuels in industrial equipment are $\lambda = 1.05 \ldots 1.15$, however, even $\lambda = 1.5$ can be realistic for some communal and domestic equipment.

3.1.1.2 Air Requirement for the Combustion of Liquid and Solid Fuels

Since both solid and liquid fuels are usually measured by weight, their combustion calculations are the same. The calculation is analogous to that of the gaseous fuels

Table 3.2 Reactions and the products derived from the combustion of liquid and solid fuel components in the case of complete combustion at air factor $n = 1$, temperature 273.15 K and pressure 101.3 kPa.

Component	Combustion Reaction	Oxygen Req. $m^3\,kg^{-1}$	Air Req. $m^3\,kg^{-1}$	Flue Gas Components $m^3\,kg^{-1}$					Flue Gas Volume $m^3\,kg–1$	
		V_{O_2}	V_{air}	V_{CO}	V_{CO_2}	V_{SO_2}	V_{N_2}	V_{H_2O}	$V_{flue,wet}$	$V_{flue,dry}$
Carbon	$C + 0.5\,O_2 \rightarrow CO$	0.93	4.44	1.87	–	–	3.51	–	–	5.38
Carbon	$C + O_2 \rightarrow CO_2$	1.87	8.89	–	1.87	–	7.02	–	–	8.89
Sulfur	$S + O_2 \rightarrow SO_2$	0.70	3.33	–	–	0.7	2.63	–	–	3.33
Hydrogen	$H_2 + 0.5\,O_2 \rightarrow H_2O$	5.60	26.60	–	–	–	21.0	11.2	32.2	–

with the exception of the volume–mass conversion. The basic combustion reactions are listed in Table 3.2.

As an example, let us examine the combustion reaction of carbon

$$C + O_2 \rightarrow CO_2 \tag{3.5}$$

1 mole of carbon requires 1 mole of oxygen. Since 1 mole of carbon weighs 12 g and 1 mole of oxygen weighs 32 g and its volume (in normal state) is 22.41 dm^3, one can easily conclude that the complete combustion of 1 kg carbon requires 22.41/12 = 1.87 m^3 oxygen. The air required for the complete combustion of 1 kg of carbon is:

$$V_{air} = 1.87 \cdot 4.76 = 8.89\,m^3kg^{-1}$$

The general equation of the theoretical (stoichiometric) air requirement of the perfect combustion of a liquid or solid fuel is, based on the stoichiometric reactions of all combustible components as shown in Table 3.2:

$$V_{air,stoich} = 4.76 \cdot \frac{1}{100}\left[\frac{22.41}{12}C + \frac{22.41}{4}H + \frac{22.41}{32}(S—O)\right] \tag{3.6}$$

that is,

$$V_{air,stoich} = 0.0476 \cdot [1.87 \cdot C + 5.6 \cdot H + 0.7 \cdot (S—O)]m^3kg^{-1} \tag{3.7}$$

In practice, the actual air supplied is usually more than the stoichiometric value (see also gas combustion) and depends on the fuel, fuel preparation and combustion technology:

$$V_{air} = \lambda \cdot V_{air,stoich} \quad m^3kg^{-1} \tag{3.8}$$

Typical values for λ for some of the common situations are:

combustion of wood	$\lambda = 1.25 \ldots 1.35$
combustion of coal, coarse	$\lambda = 1.50 \ldots 1.80$
combustion of coal, fine	$\lambda = 1.20 \ldots 1.30$
combustion of oil	$\lambda = 1.15 \ldots 1.25$

3.1.1.3 Calculations for the Case of Oxygenated Air

With the introduction of cheaper technologies for the production of oxygen, the intensification of the combustion process, and thus the technology itself, is often achieved by the use of oxygenated air.

Obviously, in this case the nitrogen to oxygen ratio is changed. For example if the oxygen content of the air is boosted to 30%, then the nitrogen content decreases to 70%. In this case the stoichiometric air volume is $100/30 = 3.33$ times the oxygen volume required for complete combustion. Thus 1 m^3 of fuel gas and 1 kg of carbon as a solid fuel, in the examples above require

$$1.75 \cdot 3.33 = 5.83\ m^3 m^{-3}$$
$$1.87 \cdot 3.33 = 6.23\ m^3 kg^{-1}$$

oxygen, respectively.

3.1.2 Calculation of the Volume and the Composition of the Flue Gas

3.1.2.1 Flue Gas of Gaseous Fuels

The volume and composition of the flue gas can be determined similarly to the calculation of the air requirement.

Let us examine again the combustion of the gas shown in the previous example. The mixture contains 85% CH_4, 10% H_2 and 5% N_2. The reaction equations are listed in Table 3.1.

It should be clear that the combustion of 1 mole of methane yields 1 mole of CO_2 and 2 moles of H_2O. The combustion of 1 mole of H_2 yields 1 mole of H_2O. Apart from CO_2 and H_2O, the flue gas will also contain nitrogen. Even though the fuel does not contain nitrogen, this component is present in the combustion air that enters the process. In the case of stoichiometric combustion of 1 m^3 fuel, the generated flue gas will contain the following components:

$$0.85\ m^3\ CO_2$$
$$2 \cdot 0.85 + 0.1 = 1.8\ m^3\ H_2O$$
$$1.75 \cdot 3.762 = 6.59\ m^3\ N_2$$

Thus the total volume of the flue gas is

$$0.85 + 1.8 + 0.05 + 6.59 = 9.29\ m^3 m^{-3}$$

The composition as a volumetric percentage is:

$$CO_2 = \frac{0.85}{9.29} 100 = 9.15\%$$

$$H_2O = \frac{1.8}{9.29} 100 = 19.40\%$$

$$N_2 = \frac{6.59 + 0.05}{9.29} 100 = 71.45\%$$

If the combustion is not stoichiometric ($\lambda = 1$), then there will also be oxygen in the flue gas because the excess oxygen simply does not react with any fuel

component and thus increases the flue gas volume. With the excess oxygen also comes excess nitrogen in the appropriate proportion.

A generalized equation for the calculation of the volume and the composition of the flue gas – using the equations of Table 3.1 – is:

Volume of the wet flue gas:

$$V_{flue,wet} = V_{CO2} + V_{H2O} + V_{O2} + V_{N2} \quad \mathrm{m^3/m^3} \tag{3.9}$$

where

$$V_{\mathrm{CO_2}} = 0.01 \cdot (\mathrm{CO_2} + \mathrm{CO} + \mathrm{CH_4} + m\mathrm{C}_m\mathrm{H}_n) \quad \mathrm{m^3 m^{-3}} \tag{3.10}$$

$$V_{\mathrm{H_2O}} = 0.01 \cdot \left(\mathrm{H_2} + \mathrm{CH_4} + \frac{n}{2} \cdot \mathrm{C}_m\mathrm{H}_n\right) \quad \mathrm{m^3 m^{-3}} \tag{3.11}$$

$$V_{\mathrm{O_2}} = 0.21 \cdot (\lambda - 1) \cdot V_{\mathrm{air,stoich}} \quad \mathrm{m^3 m^{-3}} \tag{3.12}$$

$$V_{\mathrm{N_2}} = 0.79 \cdot V_{\mathrm{air}} + 0.01 \cdot \mathrm{N_2} \quad \mathrm{m^3 m^{-3}} \tag{3.13}$$

The dry flue gas does not contain the water vapor component

$$V_{\mathrm{flue,dry}} = V_{\mathrm{N_2}} + V_{\mathrm{O_2}} + V_{\mathrm{CO_2}}\ \mathrm{m^3 m^{-3}} \tag{3.14}$$

A characteristic value for various fuels is the CO_2 content of its dry flue gas, generated under stoichiometric conditions. It is a maximum value, since fuel-lean combustion (excess air) dilutes the flue gas with O_2 and N_2, while fuel-rich (air deficient) combustion yields CO instead of some of the CO_2. This value can also be computed from the actual fuel composition

$$\mathrm{CO_{2max}} = \frac{V_{\mathrm{CO_2}}}{V_{\mathrm{CO_2}} + V_{\mathrm{N_2,stoich}}} 100\% \tag{3.15}$$

where:

$$V_{\mathrm{N_2,stoich}} = 0.79 \cdot V_{\mathrm{air,stoich}} + 0.01\mathrm{N_2 m^3 m^{-3}} \tag{3.16}$$

Typical values for CO_{2max}:

natural gas: 11.8 – 12.0%
propane-butane: 13.9 – 14.0%

3.1.2.2 Combustion Products of Liquid and Solid Fuels

The composition and volume of the flue gas is computed in an analogous manner. Thus, for wet flue gas

$$V_{flue,wet} = V_{\mathrm{CO_2}} + V_{\mathrm{H_2O}} + V_{\mathrm{SO_2}} + V_{\mathrm{O_2}} + V_{\mathrm{N_2}}\ \mathrm{m^3 kg^{-1}} \tag{3.17}$$

The amount of the individual components:

$$V_{\mathrm{CO_2}} = 0.01 \cdot 1.87\,\mathrm{C\ m^3 kg^{-1}} \tag{3.18}$$

$$V_{\mathrm{H_2O}} = 0.01 \cdot 11.2\mathrm{H} + 1.25\mathrm{H_2O\ m^3 kg^{-1}} \tag{3.19}$$

$$V_{SO_2} = 0.01 \cdot 0.7 \cdot S\ m^3kg^{-1} \tag{3.20}$$

$$V_{O_2} = 0.21 \cdot (\lambda - 1) \cdot V_{air,stoich}\ m^3kg^{-1} \tag{3.21}$$

$$V_{N_2} = 0.79 \cdot \lambda \cdot V_{air,stoich}\ m^3kg^{-1} \tag{3.22}$$

The specific volume of the dry flue gas:

$$V_{flue,dry} = V_{CO_2} + V_{SO_2} + V_{O_2} + V_{N_2}\ m^3kg^{-1} \tag{3.23}$$

The value of CO_{2max} can be determined using the same reasoning:

$$CO_{2max} = \frac{V_{CO_2}}{V_{CO} + V_{SO_2} + V_{N_2}} \tag{3.24}$$

3.1.2.3 The Effect of Oxygen Enrichment

The volume and the composition of the flue gas when oxygen enriched air is used is influenced by the actual O_2/N_2 ratio. All the rest should be trivial by now:

In the example above for the case of 30% oxygen content in the combustion air and 20% excess air ($\lambda = 1.2$) the composition of the flue gas is the following:

$0.85\ m^3\ CO_2$
$1.8\ m^3\ H_2O$
$1.75 \cdot 1.2 - 1.75 = 0.35\ m^3\ O_2$
$1,75 \cdot 1,2 \cdot 2,33 + 0.05 = 4.95\ m^3\ N_2$

The total volume of the combustion products is

$$V_{flue,wet} = 0.85 + 1.8 + 0.35 + 4.95 = 7.95\ m^3kg^{-1}$$

3.1.2.4 Effect of Temperature and Pressure (Ideal Gas Law)

This numeric value computed above is valid at normal state, that is, at the temperature $T_0 = 273.15$ K and pressure $p_0 = 101.325$ Pa. Obviously, the real temperature (and often the pressure as well) can be different than those of the normal state. Generally it is safe to assume that our gaseous components, including the flue gas, behave as an ideal gas.

The ideal gas law can be written as:

$$p \cdot V = n \cdot R \cdot T \tag{3.25}$$

where

p is the pressure (Pa),
V is the volume (m^3),
n is the amount of the gas (mol),
R is the ideal gas constant ($8.314\ J\ mol^{-1}\ K^{-1}$) and
T is the absolute temperature (K)

Thus the actual (measurable) volume of the flue gas at T_{flue} temperature and p_{flue} pressure:

$$V_{flue} = \frac{p_0}{p_{flue}} \frac{T_{flue}}{T_0} V_0 \tag{3.26}$$

Getting back to the previous example, let us calculate the actual flue gas volume at the actual temperature of 700 °C and 20 Pa overpressure:

$$V_{flue} = \frac{101.325\ \text{Pa}}{101.345\ \text{Pa}} \frac{973.15\ \text{K}}{273.15\ \text{K}} 7.95\ \text{m}^3\ \text{kg}^{-1} = 28.3\ \text{m}^3\ \text{kg}^{-1}$$

The composition by volumetric percentage is the following:

$$CO_2 = \frac{0.85}{7.95} 100 = 10.5\% \quad H_2O = \frac{1.8}{7.95} 100 = 23.2\%$$

$$O_2 = \frac{0.35}{7.95} 100 = 4.2\% \quad N_2 = \frac{4.95}{7.95} 100 = 62.1\%$$

The composition of an ideal gas mixtures does not change due to temperature or pressure variation, unless dissociation reactions are considered at the examined (e.g., flame) temperature.

Thus increasing the oxygen content in the air decreases the flue gas volume (and consequently the adiabatic flame temperature, as we will see soon).

3.1.2.5 Determination of the Actual Excess Air Factor

In order to examine the actual burning process, measurements are needed on the composition of the flue gas generated. From the actual measurements, one can calculate the real excess air factor. For this one should use the dry flue gas composition as most of the flue gas analyzers provide direct data on dry flue gas.

The following equation is based on the nitrogen balance of the fuel, combustion air and the flue gas, as well as on the excess O_2 content, appearing in the flue gas.

In the case of solid and liquid fuels the calculation is based on the nitrogen content provided by the stoichiometric and actual (real) combustion air volume.

$$\lambda = \frac{V_{air}}{V_{air,stoich}} = \frac{N_2}{N_2 - \frac{79}{21} O_2} = \frac{1}{1 - 3.762 \frac{O_2}{N_2}} \tag{3.27}$$

Most of the gaseous fuels already contain nitrogen, thus the fuel nitrogen must be taken into account in excess of the flue gas nitrogen:

$$\lambda = \frac{V_{air}}{V_{air,stoich}} = \frac{N_2 - \frac{N_{2,fuel}}{V_{flue,dry}}}{\left(N_2 - \frac{N_{2,fuel}}{V_{flue,dry}}\right) - 3.762 O_2} = \frac{1}{1 - 3.762 \frac{O_2}{N_2 - \frac{N_{2,fuel}}{V_{flue,dry}}}} \tag{3.28}$$

Incomplete combustion yields CO_2, CO, H_2, H_2O and N_2 components in the flue gas. The oxygen consumption decreases by $0.5(CO + H_2)$, thus the air volume changes by

$$\frac{4.76}{2}(CO + H_2) \tag{3.29}$$

while the nitrogen content changes by

$$\frac{3.76}{2}(CO + H_2) \tag{3.30}$$

The real excess air factor in this case can be calculated as:

$$\lambda = \frac{N_2}{N_2 - 3.76\left(O_2 - \frac{CO}{2} - \frac{H_2}{2}\right)} \tag{3.31}$$

3.1.3
Determination of the Combustion Temperature

If all of the heat generated by the combustion of a fuel is absorbed by the generated flue gas, then the flue gas reaches its theoretical combustion temperature. The calculation is based on a simple heat balance of an adiabatic combustion process, therefore this temperature is also called the adiabatic flame temperature.

$$T_{ad} = \frac{LHV}{V_{flue,wet} \cdot c_{p,flue}} {}^{\circ}C \tag{3.32}$$

Where LHV is the lower heating value of the fuel, [kJ m^{-3}, kJ kg^{-1}], $V_{flue,wet}$ is the flue gas volume per unit amount of fuel, [m^3 m^{-3}, m^3 kg^{-1}] and $c_{p,flue}$ is the average specific heat capacity of the flue gas at the combustion temperature, [kJ m^{-3} °C^{-1})]

If the fuel and/or the combustion air are/is preheated, their heat content cannot be neglected. Thus:

$$T_{ad} = \frac{LHV + Q_{phys}}{V_{flue,wet} \cdot c_{p,flue}} \tag{3.33}$$

here the physical heat content of the fuel and the air is

$$Q_{phys} = \lambda \cdot V_{air,stoich} \cdot T_{air} \cdot c_{p,air} + T_{fuel} \cdot c_{p,fuel}\ kJm^{-3}\ (kJ\ kg^{-1}) \tag{3.34}$$

The specific heat content of the gas mixture can be calculated according to the simple mixing rule:

$$c_{p,fuel} = c_{p,CO_2} \cdot CO_2 + c_{p,H_2O} \cdot H_2O + c_{p,N_2} \cdot N_2 + \ldots \tag{3.35}$$

Heat capacity values for air and various components are listed in various technical tables as a function of temperature.

Besides the specific heat capacities, one can also use the enthalpy that is actually the product of the specific heat capacity and the temperature.

$$h = c_p \cdot T \,\mathrm{kJm^{-3}} \tag{3.36}$$

Enthalpy values for various gases as a function of temperature are listed similarly in tables. The enthalpy of mixtures can be calculated by the mixing rule, as was the case for the specific heat capacity.

Since the specific heat capacity of gases is a function of the temperature and the temperature of combustion is to be computed, the computation usually requires an iterative approach.

Let us compute the theoretical adiabatic temperature of our gas mixture from the examples above.

The composition of the fuel is 85% CH_4, 10% H_2 and 5% N_2. Combustion is stoichiometric, thus the excess air factor is $\lambda = 1$.

Enthalpy of the combustion products:

$$h_0 = c_p \cdot T_{\mathrm{ad}} = \frac{\mathrm{LHV}}{V_{\mathrm{flue,wet}}} = \frac{31605}{9.29} = 3410\,\mathrm{kJm^{-3}}$$

An engineering guess for the flame temperature: $T_{\mathrm{ad}} = 2100\,^{\circ}\mathrm{C}$ (2373 K).

At this temperature the enthalpies of the flue gas components are:

$$\begin{aligned} h_{\mathrm{CO_2}} &= 0.0915 \cdot 5186.81 = 474.5\,\mathrm{kJm^{-3}} \\ h_{\mathrm{H_2O}} &= 0.194 \cdot 4121.79 = 800.1\,\mathrm{kJm^{-3}} \\ h_{\mathrm{N_2}} &= 0.7145 \cdot 3131.96 = 2232.0\,\mathrm{kJm^{-3}} \\ \hline h_{2100} &= \qquad\qquad 3506.6\,\mathrm{kJm^{-3}} \end{aligned}$$

Since $h_0 < h_{2100}$, the real temperature is most probably smaller than 2100 °C. Let us iterate over the temperature and assume now $T_{\mathrm{ad}} = 2000\,^{\circ}\mathrm{C}$. The enthalpies in this case are:

$$\begin{aligned} h_{\mathrm{CO_2}} &= 0.0915 \cdot 4910.51 = 449.7\,\mathrm{kJm^{-3}} \\ h_{\mathrm{H_2O}} &= 0.194 \cdot 3889.72 = 754.8\,\mathrm{kJm^{-3}} \\ h_{\mathrm{N_2}} &= 0.7145 \cdot 2970.25 = 2120.0\,\mathrm{kJm^{-3}} \\ \hline h_{2100} &= \qquad\qquad 3324.5\,\mathrm{kJm^{-3}} \end{aligned}$$

Since now $h_{2000} < h_0$, the real flame temperature must be between 2000 and 2100 °C. We can either iterate one more step or simply interpolate by the enthalpy values.

$$T_{\mathrm{ad}} = 2000 + \frac{3410 - 3324.5}{3506.6 - 3324.5}100 = 2047\,^{\circ}\mathrm{C}$$

For flame temperatures above 1800 °C, the effect of dissociation must also be accounted for. This phenomenon is based on the experience that both the CO_2 and the H_2O can disintegrate into oxygen as well as CO and H_2, respectively. Taking this effect into consideration our last and most exact equation for the flame temperature is the following

$$T_{ad} = \frac{LHV + Q_{phys} - Q_{diss}}{V_{flue,wet,dis} \cdot c_{p,flue}} °C \tag{3.37}$$

where

Q_{diss} is the dissociation heat from the disintegration of the flue gas CO_2 and H_2O.

Above 1500 °C a noticeable, and above 1800 °C a non-negligible dissociation occurs with the three atom components of the flue gas. These reactions are essentially the reverse of the combustion reactions and thus require heat that is equal to the heat generated in the forward reactions. The heat consumption results in decreasing flame temperature. The reactions are the following:

$$2CO_2 \rightarrow 2CO + O_2 \quad \text{with a heat consumption of} = 12645\,kJm^{-3}CO_2$$
$$2H_2O \rightarrow 2H_2 + O_2 \quad \text{with a heat consumption of} = 10760\,kJm^{-3}H_2O$$

The percentage of dissociation can be expressed with the following equations:

$$a = \frac{V_{CO_2diss}}{V_{CO_2}} \cdot 100 \tag{3.38}$$

and

$$b = \frac{V_{H_2Odiss}}{V_{H_2O}} \cdot 100 \tag{3.39}$$

that can be calculated from the reaction rate constants and the partial pressure values.

The rate of dissociation can be computed from the graphs shown in Figure 3.2 for CO_2 and Figure 3.3 for H_2O. Both graphs show the rates as a function of the temperature and the partial pressure.

The rate of dissociation can then be used to compute the heat effect of the reactions:

$$Q_{diss} = a \cdot V_{CO_2} \cdot 12\,645 + b \cdot V_{H_2O} \cdot 10\,760\,kJ\,m^{-3} \tag{3.40}$$

where $V_{CO_2}$and V_{H_2O} are the specific volumes of CO_2 and H_2O, respectively in $m^3\,m^{-3}$.

The theoretical (adiabatic) flame temperature cannot be achieved in real combustion applications. This is because for ignition and combustion time is

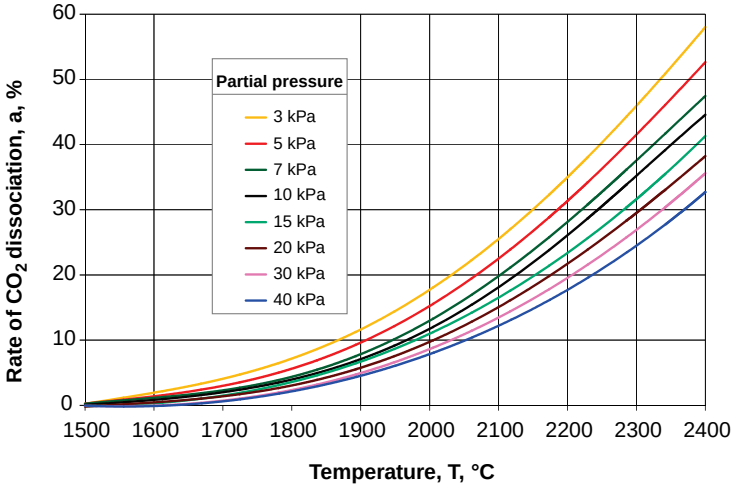

Figure 3.2 Rate of CO_2 dissociation as a function of temperature and partial pressure.

needed, and during this finite time the flame having a surface in space releases some of its heat to the environment. The real flame temperature is always lower than the theoretical one.

Through the intensification of mixing, the combustion process can be accelerated and thus the heat loss from the flame can be minimized. In this way the real flame

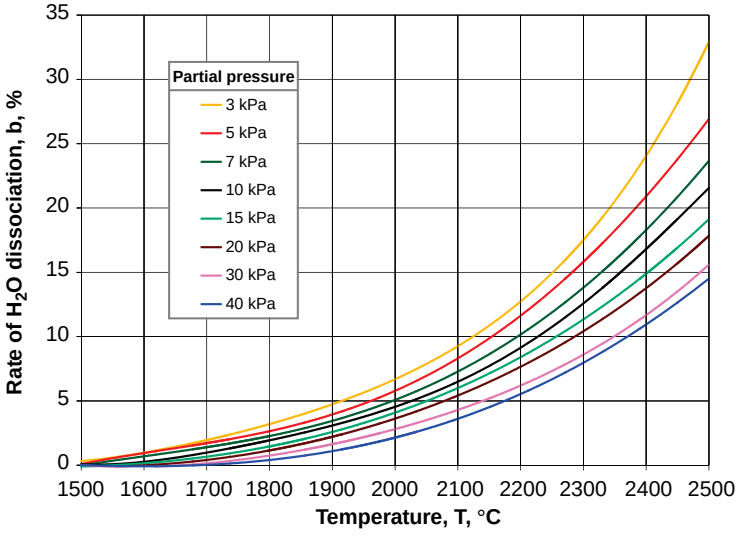

Figure 3.3 Rate of H_2O dissociation as a function of temperature and partial pressure.

temperature can approach the adiabatic flame temperature. The ratio of these temperature values is defined as the pyrometric efficiency:

$$\eta_{\text{pyr}} = \frac{T_{\text{flame,measured}}}{T_{\text{ad,theoretical}}} \tag{3.41}$$

The pyrometric efficiency, depending on the conditions of combustion, can vary between 0.65 and 0.85. For tunnel furnaces the value is approximately 0.80, for shaft kilns, 0.70, for rotary kilns, 0.70–75.

3.1.4 Heating Values

Heating values (calorific values) can be computed from the composition of the fuel. Only the combustible components should be taken into account. The calculation is done using the simple mixing rule for solid, liquid and gaseous fuels.

For solid and liquid fuels the composition is based on weight, thus the higher heating value (HHV) can be computed, from the carbon, hydrogen, sulfur and water content. The latter is important, because if the water content of the flue gas leaves the system in vapor form, the vaporization heat is lost, therefore the useful heat is less than the theoretical HHV. Using ultimate and proximate analysis results, the lower heating value (LHV) can be calculated as follows (composition values must be provided in weight fraction):

$$\text{LHV} = 33440 \cdot \text{C} + 115300 \cdot \text{H} + 9279 \cdot \text{S} - 2440 \cdot \text{H}_2\text{O} \ \text{kJ kg}^{-1} \tag{3.42}$$

If the HHV is given from laboratory measurement (bomb calorimetry), then the lower heating value can be calculated from the higher heating value, the fuel's hydrogen and moisture content, and the heat of water evaporation:

$$\text{LHV} = \text{HHV} - 2440 \cdot (9 \cdot \text{H} + \text{H}_2\text{O}), [\text{kJ kg}^{-1}] \tag{3.43}$$

where HHV is the higher heating value of the fuel (kJ kg^{-1}), H is the hydrogen content in weight fraction, H_2O is the water (moisture) content in weight fraction.

For gaseous fuels – since the reactants, the oxidizer and the reaction products are all gaseous – the calculation is even more straightforward. Since the fuels gas usually does not contain moisture directly, all water content must come from the hydrogen containing components. Using experimental data for the various combustible components the lower heating value can be computed using the following formula:

$$\begin{aligned}\text{LHV} = {} & 33940 \cdot \text{CH}_4 + 60799 \cdot \text{C}_2\text{H}_6 + 88438 \cdot \text{C}_3\text{H}_8 + 111042 \cdot \text{C}_4\text{H}_{10} \\ & + 137227 \cdot \text{C}_5\text{H}_{12} + 160949 \cdot \text{C}_6\text{H}_{14} + 57069 \cdot \text{C}_2\text{H}_4 + 53973 \cdot \text{C}_2\text{H}_2 \\ & + 10257 \cdot \text{H}_2 + 12048 \cdot \text{CO} \ \text{kJm}^{-3}\end{aligned} \tag{3.44}$$

3.1.5
Laminar Flame Velocity

The laminar flame velocity is affected by the physical conditions of the combustion process, that is, burning characteristics of the fuel, air ratio, gas and air temperature, inert (CO_2, N_2) content, and the furnace temperature (via ignition time).

Let us calculate the laminar flame velocity of a natural gas fired flat flame burner.

Known parameters:

Excess air factor: $\lambda = 1.05$
Natural gas composition: 90% CH_4, 5% CO_2, 5% N_2
Gas temperature: $T_{\text{fuel}} = 293\,\text{K}$
Air temperature: $T_{\text{air}} = 773\,\text{K}$
Heat capacities: $c_{p,O_2} = 1.52\,\text{kJ m}^{-3}\,\text{K at } 293\,\text{K}$
$c_{p,CO_2} = 2.26\,\text{kJ m}^{-3}\,\text{K at } 293\,\text{K}$
$c_{p,CH_4} = 1.88\,\text{kJ m}^{-3}\,\text{K at } 293\,\text{K}$
$c_{p,H_2O} = 1.77\,\text{kJ m}^{-3}\,\text{K at } 293\,\text{K}$
$c_{p,N_2} = 1.42\,\text{kJ m}^{-3}\,\text{K at } 293\,\text{K}$
$c_{p,\text{air}} = 1.293\,\text{kJ m}^{-3}\,\text{K at } 773\,\text{K}$

The calculation includes three steps:

1) Since the only combustible component in the fuel is methane, the first order estimate of the normal flame velocity of our fuel would be the value for CH_4 at the appropriate excess air. From Figure 3.4 at $\lambda = 1.05$ the CH_4 normal flame velocity is

$$w_0 = 0.38\,\text{m s}^{-1}$$

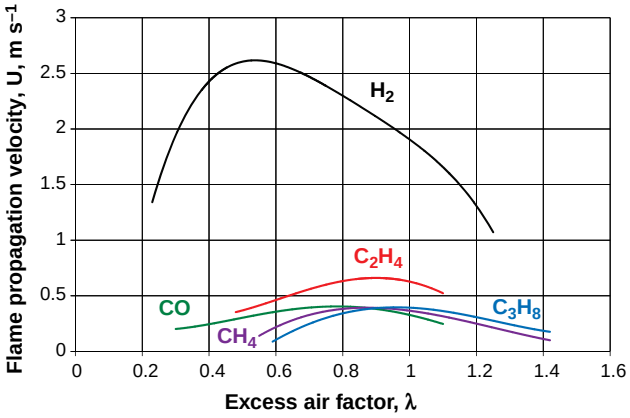

Figure 3.4 Laminar flame velocity as a function of the excess air.

2) Since our fuel contains non-combustible components, this inert gas content decreases the flame speed:

$$\begin{aligned} w &= w_0 \cdot (1 - 0.8 \cdot \mathrm{N_2} - 1.6 \cdot \mathrm{CO_2} - 3 \cdot \mathrm{O_2}) \\ &= 0.38 \cdot (1 - (0.8 \cdot 0.05) - (1.6 \cdot 0.05)) = 0.33\,\mathrm{m\,s^{-1}} \end{aligned} \tag{3.45}$$

3) The temperature of the fuel–air mixture increases the flame speed.

Let us calculate the temperature of the mixture first, by using the appropriate heat capacity values from the tabular values of the components:

$$\begin{aligned} c_{p,\mathrm{fuel}} &= \mathrm{CH_4} \cdot c_{p,\mathrm{CH_4}} + \mathrm{CO_2} \cdot c_{p,\mathrm{CO_2}} + \mathrm{N_2} \cdot c_{p,\mathrm{N_2}} \\ &= 0.9 \cdot 1.88 + 0.05 \cdot 2.26 + 0.05 \cdot 1.42 = 1.87\,\mathrm{kJ\,m^{-3}K^{-1}} \end{aligned} \tag{3.46}$$

The heat capacity of the fuel-air mixture can be calculated by taking the respective volumes into consideration:

$$\begin{aligned} c_{p,\mathrm{mix}} &= (V_{\mathrm{fuel}} \cdot c_{p,\mathrm{fuel}} + V_{\mathrm{air}} \cdot c_{p,\mathrm{air}})/(V_{\mathrm{fuel}} + V_{\mathrm{air}}) \\ &= (1 \cdot 1.87 + 10 \cdot 1.293)/(1 + 10) = 1.35\,\mathrm{kJ\,m^{-3}K^{-1}} \end{aligned} \tag{3.47}$$

Thus the temperature of the mixture can be calculated:

$$\begin{aligned} T_{\mathrm{mix}} &= (T_{\mathrm{fuel}} \cdot c_{p,\mathrm{fuel}} \cdot V_{\mathrm{fuel}} + T_{\mathrm{air}} \cdot c_{p,\mathrm{air}} \cdot V_{\mathrm{air}})/(c_{p,\mathrm{mix}} \cdot V_{\mathrm{mix}}) \\ &= ((293 \cdot 1.87 \cdot 1) + (773 \cdot 1.293 \cdot 10))/(1.35 \cdot 11) = 707\,\mathrm{K} \end{aligned} \tag{3.48}$$

The temperature effect can be considered as follows:

$$\begin{aligned} w_{\mathrm{real}} &= w \cdot (T_{\mathrm{mix}}/T_0)^{1.8} \\ &= 0.33 \cdot (707/293)^{1.8} = 1.89\,\mathrm{m\,s^{-1}} \end{aligned} \tag{3.49}$$

The actual flame propagation velocity at the given conditions for this furnace is $1.89\,\mathrm{m\,s^{-1}}$, a fairly high value.

3.2
Heat-, Mass- and Momentum Transport and Balance

3.2.1
Transport

Transport is the basis for combustion and chemical reaction in general. Species have to be brought together, so that they can react with each other. However, there exist different transport mechanisms for the species and also transport mechanisms for heat as well as for the momentum. It is established that a concentration gradient leads to mass transport, called diffusion, and temperature gradients lead to heat transport, called heat conduction. Transport phenomena of mass, momentum and heat have notable analogies in their mathematical formulations; that means in the structure of their differential equations.

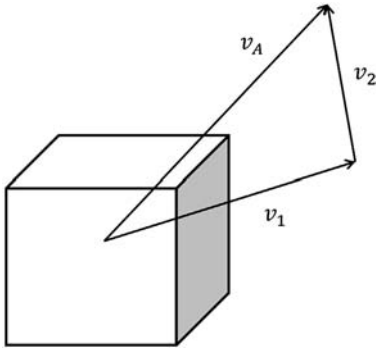

Figure 3.5 The transports mechanisms of convective and diffusive transport. Velocity vectors: $\vec{v}_1$ is the mass average velocity. $\vec{v}_2$ is the mass diffusion velocity. $\vec{v}_A$ is the velocity of species A.

3.2.2 Mass Transport

There are two main processes occurring when various different chemical species appear in a mixture. They cause the transport characteristics in this mixture. The two mechanisms which contribute to these transport processes are diffusion and convection.

Figure 3.5 shows the velocity vectors of a chemical species.

$$\vec{v}_\mathrm{A} = \vec{v}_1 + \vec{v}_2 \tag{3.50}$$

3.2.2.1 Diffusive Mass Transport

Concentration differences lead to the diffusion of the species. The driving force is the concentration gradient and this is used in Fick's first law. It describes the molar or mass flow which is proportional to the concentration gradient. The Fick's first law of a binary system including species A and B is shown in Eq. (3.51) below. $\vec{\dot{N}}_\mathrm{A}$ is the molar flow of species A in $\mathrm{mol\,s^{-1}}$, D_AB is the diffusion coefficient of the binary system of A and B in $\mathrm{m^2\,s^{-1}}$, A is the area of consideration and $\frac{\mathrm{d}\vec{c}_\mathrm{A}}{\mathrm{d}x}$ is the molar concentration gradient of species A in $\mathrm{mol\,m^{-4}}$.

$$\vec{\dot{N}}_\mathrm{A} = -D_\mathrm{AB} \cdot A \cdot \frac{\mathrm{d}\vec{c}_\mathrm{A}}{\mathrm{d}x}\ \mathrm{mol\,s^{-1}} \tag{3.51}$$

In order to explain how one can imagine a three-dimensional concentration distribution it is shown in Figure 3.6. With time the concentration peak will decrease due to its diffusion.

3.2.2.2 Convective Mass Transport

Due to a flow, for example, because a pump is used (forced convection) the species are transported with their velocity.

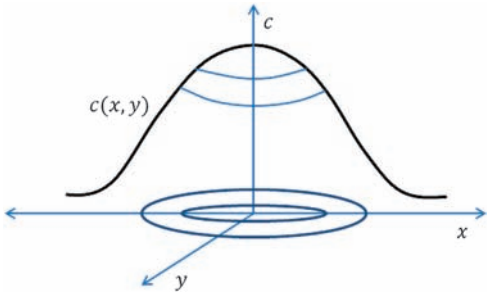

Figure 3.6 The concentration gradient at a certain time step in space.

Equation (3.52) describes the convective transport of species A, in which $\vec{m}_{\mathrm{A,conv}}$ is the mass flow vector, ρ_{A} the density of the matter and $\vec{v}_1$ the velocity vector.

$$\vec{m}_{\mathrm{A,conv}} = \rho_{\mathrm{A}} \vec{v}_1 \ \mathrm{kg\,s^{-1}\,m^{-2}} \tag{3.52}$$

3.2.3 Mass Transfer

The mass transfer is based on a concentration difference and is described in Eq. (3.53). $\dot{N} = \beta \cdot A \cdot (c_{\mathrm{A},1} - c_{\mathrm{A},2})$ is the molar flow of species A in mol $\mathrm{s^{-1}}$ and based on diffusive and convective transport mechanisms. Figure 3.7 shows a concentration profile of species A in combination with the velocity profile of the flow. A concentration boundary layer is formed.

$$\dot{N} = \beta \cdot A \cdot (c_{\mathrm{A},1} - c_{\mathrm{A},2}) \ \mathrm{mol\,s^{-1}} \tag{3.53}$$

where β is the mass transfer coefficient in $\mathrm{m\,s^{-1}}$, A is the area of exchange in $\mathrm{m^2}$, $c_{\mathrm{A},1}$ and $c_{\mathrm{A},2}$ are the different molar concentrations of species A in $\mathrm{mol\,m^{-3}}$.

A basic method to find the mass transfer coefficient β is the experiment. The use of similarity or model theory can reduce the number of experiments significantly.

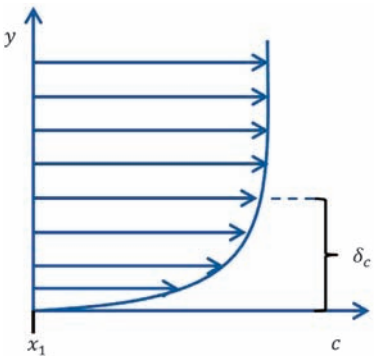

Figure 3.7 Concentration profile in a flow: δ_c shows the concentration boundary layer. Arrows indicate the velocity of the flow.

The solution of a physical problem will be independent of any unit and it can be represented by dimensionless variables.

To calculate the dimensionless parameters, the parameters are related to their corresponding characteristic parameters, for example, characteristic length (L_0) or characteristic concentration (c_0).

The Sherwood number will be calculated as below, where L_0 is the characteristic length and D_{AB} is the diffusion coefficient in $m^2\,s^{-1}$.

$$Sh = \frac{\beta \cdot L_0}{D_{AB}} \tag{3.54}$$

The Sherwood number (Sh) relates the total mass transfer to the diffusion and is a function of the Reynolds number (Re) and the Schmidt number (Sc). With the Sherwood number the mass transfer coefficient (β) can be calculated.

The Reynolds number is given by:

$$Re = \frac{V \cdot L_0}{\nu} \tag{3.55}$$

V is the characteristic velocity in $m\,s^{-1}$ and ν is the kinematic viscosity in $m^2\,s^{-1}$.

It can also be defined as the ratio of inertial forces to viscous forces.

The Schmidt number is given by:

$$Sc = \frac{\nu}{D_{AB}} \tag{3.56}$$

and relates the viscous diffusion rate to the mass diffusion rate.

3.2.4 Heat Transport

In order to characterize the mechanisms of heat transfer, three models are described. These are thermal conduction, convection and thermal radiation. By analogy with mass transfer, the transfer of heat takes place by diffusion and is called thermal conduction. Thermal radiation is not bounded to matter and can also appear in vacuum systems.

3.2.4.1 Heat Conduction

Equation (3.57) is known as Fourier's law and describes heat conduction. $\vec{\dot{q}}_{conduction}$ is the heat flux in [$W\,m^{-2}$], λ the thermal conductivity in [$W\,m^{-1}\,K^{-1}$] and $\frac{\partial \vec{T}}{\partial x}$ is the temperature gradient in [$K\,m^{-1}$].

$$\vec{\dot{q}}_{conduction} = -\lambda \cdot \frac{\partial \vec{T}}{\partial x} \tag{3.57}$$

The thermal conductivity λ can be described as the ability of a material to conduct heat.

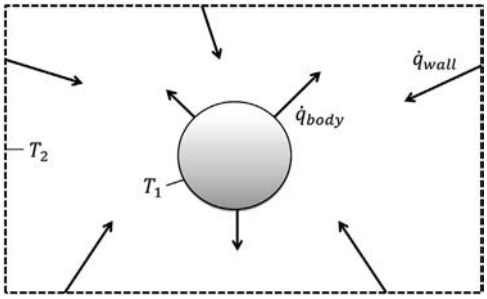

Figure 3.8 Radiation of a body at temperature T_1 in its surroundings with temperature T_2.

3.2.4.2 **Thermal Radiation**

In order to transport the energy by convection and conduction, a matter is required, but radiation does not need a material connection. When a body emits radiation, it is the internal energy that turns into electromagnetic waves. Gases and liquids absorb and emit the radiation inside their space, but solids absorb it within a thin layer of their surface (Figure 3.8).

Stefan–Boltzmann's law shows the maximum possible heat flux. This emitter is called a black body. $\dot{q}_{\text{radiation}}$ in $\mathrm{W\,m^{-2}}$ shows the black body radiation flux, σ is the Stefan–Boltzmann constant which is $5.67 \times 10^{-8}\ \mathrm{W\,m^{-2}\,K^{-4}}$], T the temperature in K.

$$\dot{q}_{\text{black body}} = \sigma.T^4 \tag{3.58}$$

The black body is an ideal absorber and ideal emitter.

The emissive power of real radiators can be described by using a correction factor. ε is the emissivity factor.

For a black body $\varepsilon = 1$.

$$\dot{q} = \varepsilon \cdot \sigma \cdot T^4 \tag{3.59}$$

When radiation hits a body, some of it will be reflected, some absorbed and some transmitted (refer also to Figure 3.9).

$$r + a + t = 1 \tag{3.60}$$

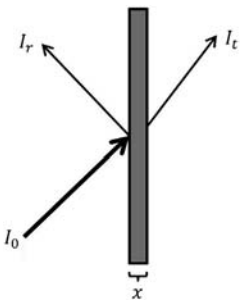

Figure 3.9 Radiation with an intensity of I_0 hits a body and is partly reflected (I_r), partly transmitted (I_t)and partly absorbed (not shown).

Where r is the reflectivity and is equal to $\frac{I_r}{I_0}$, a is the absorptivity and is equal to $= 1 - r - t$, and t is the transmissivity and equal to $t = \frac{I_t}{I_0}$.

The heat which is transmitted by radiation between two subjects happens not only from the subject at the higher temperature to the other one, but also from the cooler subject to the hotter. The net heat flow from the hotter subject to the body at lower temperature is of interest. The heat flow which is emitted by the radiator can be calculated with:

$$\dot{q}_{em} = \varepsilon \cdot \sigma \cdot T_1^4 \tag{3.61}$$

The heat absorbed by the radiator is described by Eq. (3.62), where a is the absorptivity of the radiator.

$$\dot{q}_{ab} = a \cdot \sigma \cdot T_2^4 \tag{3.62}$$

For a gray body it is assumed that $\varepsilon = a$.

The net heat flow is calculated using Eq. (3.63).

$$\dot{q}_{radiation} = \dot{q}_{em} - \dot{q}_{ab} = \varepsilon \cdot \sigma \cdot (T_1^4 - T_2^4) \tag{3.63}$$

In many applications heat transfer by convection and conduction must be considered in addition to the radiative heat transfer.

$$\dot{q} = \dot{q}_{cond.+conv.} + \dot{q}_{radiation} \tag{3.64}$$

$$\dot{q} = \alpha \cdot (T_1 - T_2) + \varepsilon \cdot \sigma \cdot (T_1^4 - T_2^4) \tag{3.65}$$

where α is the heat transfer coefficient for the convective and conductive heat transfer in $\mathrm{W\,m^{-2}\,K^{-1}}$, refer also to Section 3.2.5.

Electromagnetic waves (Figure 3.10) spread out in a straight line at the speed of light (c_0) $3.00 \times 10^8\,\mathrm{m\,s^{-1}}$ in vacuum. In a medium, while their frequency f remains unchanged, the velocity is lower than c_0.

The equation relating the wavelength λ in m and the frequency f in $\mathrm{s^{-1}}$ is:

$$c = \lambda \cdot f \tag{3.66}$$

The radiation reduces its energy when it passes through a gas or mixture of gases. This phenomenon happens because of the absorption and scattering of the

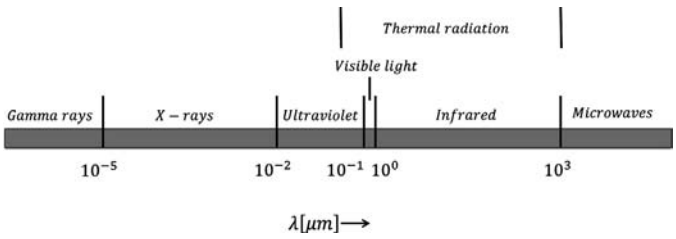

Figure 3.10 The electromagnetic wave spectrum showing the area of thermal radiation.

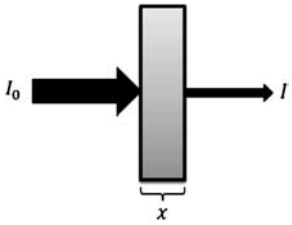

Figure 3.11 The absorption of the incident beam with intensity I_0. passing through a gas with a width of x in m, refer to Lambert–Beer's law.

waves through the gas molecules. If we assume that the radiation is only absorbed but not scattered, Lambert–Beer's law describes the reduction of the incident beam with an intensity of I in $\mathrm{W\,m^{-2}}$ with increasing length x in m of the beam in the gas (Figure 3.11).

$$\frac{\mathrm{d}I}{\mathrm{d}x} = -k \cdot I \tag{3.67}$$

$$k = k' \cdot c \tag{3.68}$$

where k is the spectral absorption coefficient of the absorbing gas in $\mathrm{m^{-1}}$,which also depends on the concentration of the absorbing gas c in $\mathrm{mol\,m^{-3}}$. k' is the spectral absorption coefficient in $\mathrm{m^2\,mol^{-1}}$.

Integration of Eq. (3.67) between $x = 0$ and x yields:

$$I = I_0 \cdot \mathrm{e}^{-k \cdot x} \tag{3.69}$$

The amount of absorbance (A) can be calculated as follows:

$$A = \ln \frac{I_0}{I} = k' \cdot c \cdot x \tag{3.70}$$

The Lambert–Beer law is used as the basis for quantitative absorption spectroscopy.

In Figure 3.12 the radiation spectra of black bodies at different temperatures can be seen according to Planck's law. A radiation spectrum of a black body undergoes a maximum. The higher the temperature, the higher the total radiation according to the Stefan–Boltzmann law.

The maximum value of the wavelength of the radiation spectra show a maximum value which is described by Wien's displacement law:

$$\lambda_{\max} \cdot T = 2897\ \mu\mathrm{m\ K} \tag{3.71}$$

The higher the temperature of the object, the more its radiation maximum $\lambda_{\max}$, in μm, is shifted to lower wavelengths.

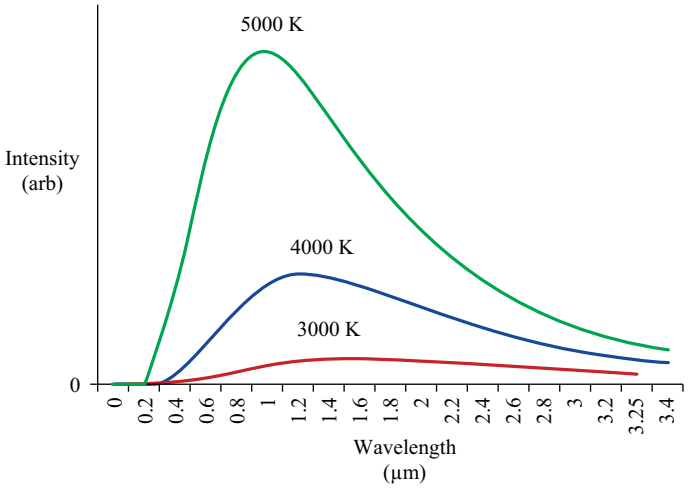

Figure 3.12 The radiation spectrum of a black body according to Planck's law for different temperatures.

3.2.5
Heat Transfer

While a fluid is flowing, the heat transfer $\dot{Q}$ (W m^{-2}) is by heat conduction due to the temperature gradient and by the movement of the fluid (convection). This is described by Eq. (3.72). (However, heat transfer by radiation may also be of importance, refer to Section 3.2.4.2.)

$$\dot{Q} = \alpha \cdot A \cdot (T_1 - T_2) \tag{3.72}$$

where α is the heat transfer coefficient in W m^{-2} K^{-1}, A is the area in m^2 and $T_1 - T_2$ is the temperature difference in K between the media.

Similar to the mass transfer case, where the flow affects the concentration boundary layer (see Figure 3.7), the temperature boundary layer is also affected and the heat transfer coefficient. Figure 3.13 shows the heat transfer between a sphere and its surrounding flow. The heat transfer coefficient is obtained from the dimensionless Nusselt number (Nu).

$$Nu = \frac{\alpha \cdot L_0}{\lambda} \tag{3.73}$$

where L_0 is the characteristic length in m and λ is the thermal heat conductivity in W m^{-1} K^{-1}.

The Nusselt number compares the convective heat transfer to the conductive heat transfer through the temperature boundary layer and is mainly a function of the

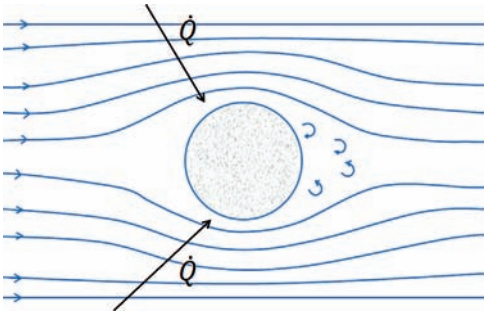

Figure 3.13 Sketch showing the heat transfer between a sphere and its surrounding flow.

Reynolds number (*Re*) and the Prandtl number (*Pr*) which is given by

$$Pr = \frac{\mu \cdot c_p}{\lambda} = \frac{\nu}{a} \tag{3.74}$$

$$a = \frac{\lambda}{c_p \cdot \varrho} \tag{3.75}$$

where μ is the dynamic viscosity in Pa s, a is the thermal diffusivity in $m^2\,s^{-1}$, c_p is the specific heat capacity in $J\,kg^{-1}\,K^{-1}$, λ is the thermal heat conductivity in $W\,m^{-1}\,K^{-1}$, and ϱ is the density of the fluid in $kg\,m^{-3}$.

As an example, the Nusselt number of a sphere or spherical particle in a flow of gas or liquid is obtained by the following equation:

$$Nu = 2 + 0.6\, Re^{\frac{1}{2}} Pr^{\frac{1}{3}} \tag{3.76}$$

3.2.6
Momentum Transport

The momentum (P) of a mass-carrying particle is a physical property and is formed by the product of mass (m in kg) and velocity (v in $m\,s^{-1}$) of the particle. In a closed system the momentum is subject to the conservation law.

$$P = m.v \tag{3.77}$$

Viscosity is a physical property of fluids caused by internal friction. In order to make viscosity comprehensible, an experiment is presented. A plate on a lake is moving constantly with velocity v and the flow profile shown in Figure 3.14 will be obtained after a certain time period, that is, after acceleration.

Due to adherence at the wall, the fluid at the plate has the same velocity as the plate itself.

In dealing with flow problems, the flow type used determines the flow characteristics and phenomena. The most common fluids used in chemistry and technique are water and air and represent Newtonian fluids. They fulfill the Newton's law of viscosity, which

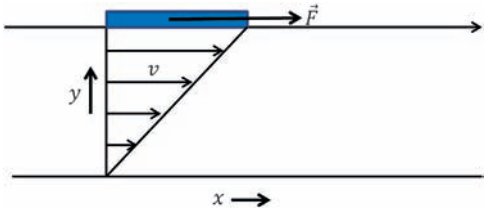

Figure 3.14 Velocity profile below a plate which is constantly drawn with force *F* over a lake.

is formulated in Eq. (3.78) where τ_{xy} is the shear force per unit area in Pa, ν is the kinematic viscosity in $m^2\,s^{-1}$, ρ the density and $\frac{\partial \vec{v}}{\partial y}$ the velocity gradient in s^{-1}.

$$\vec{\tau}_{xy} = -\nu \cdot \rho \cdot \frac{\partial \vec{v}}{\partial y} \tag{3.78}$$

This law states that the shearing force is proportional to the shear rate, whereas the proportionality is a property of the fluid and is defined as dynamic viscosity. The correlation between dynamic and kinematic viscosity is given in Eq. (3.79) where μ is the dynamic viscosity.

$$\nu = \frac{\mu}{\rho} \tag{3.79}$$

There are other types of flow laws which are illustrated in Figure 3.15. Non-Newtonian fluids do show a more complicated correlation between shear stress and shear strain rate.

Typical examples of some non-Newtonian fluids are:

- Bingham plastics are rigid bodies when no or low stress is applied, but flow like a viscous fluid at high stress. For example, toothpaste.
- Dilatant (shear thickening) fluids' viscosity increases with the rate of shear strain. For example, sand + water.
- Pseudoplastic (shear thinning) fluids' viscosity decreases with the rate of shear strain. For example, fibrous solutions.

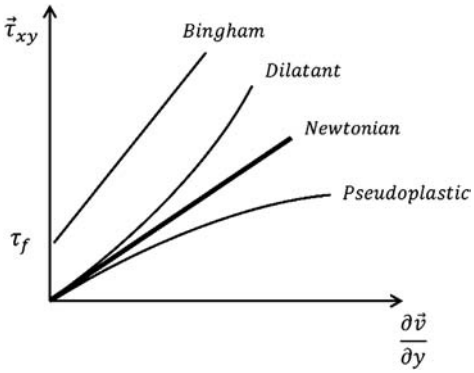

Figure 3.15 Flow characteristics of different media.

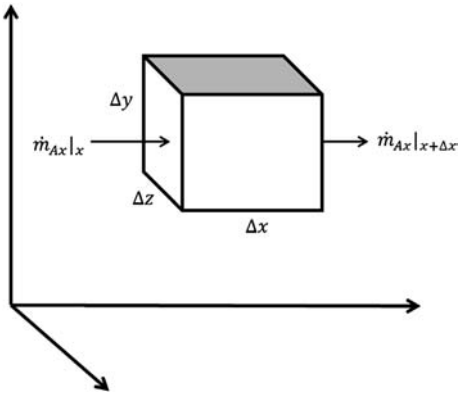

Figure 3.16 Balance space as a finite volume. $\dot{m}_{Ax}$ is the mass flow of species A based on area in kg $s^{-1} m^{-2}$.

3.2.7 Balance

In order to get balance equations for mass, energy or momentum, a balance volume, sketched in Figure 3.16, has to be defined.

The balance volume is enclosed by a real or imaginary surface, whereas macroscopic or microscopic mass, energy or momentum flows can pass through. In the case of temporal changing conditions, the balance is formed in general as follows:

$$\text{Temporal Change} = \text{Input} - \text{Output} \pm \text{Source/Sink} \tag{3.80}$$

There are four terms which are taken into account when balance equations are put together: The temporal change gives the total change within the finite volume in time. It can be an increase (e.g., in terms of mol s^{-1} for a species balance or in J s^{-1} for a heat balance) or a decrease, or it can be constant or zero. If it is zero then a steady state is given. The input gives the total input into the finite volume, for example, the input of species A or heat in time. The output gives the total output out of the finite volume. The source term or sink term represents, for example, the formation of species by chemical reaction in a species balance (mol s^{-1}) or the heat of formation of a chemical reaction in the heat balance (J s^{-1}).

Equation (3.80) leads to a mass balance when applied to a concentration field, to a heat balance when applied to a temperature field, and to a momentum balance when applied to a velocity field.

3.2.7.1 Mass Balance

We assume that we have a binary system, consisting of the species A and B. According to Eq. (3.80), the mass balance is calculated as:

$$\text{Temporal change}: \quad \frac{\partial \rho_A}{\partial t} \Delta x \Delta y \Delta z \, \text{kg s}^{-1} \tag{3.81}$$

$$\text{Input of A in } x \text{ direction} : \dot{m}_{Ax}|_x \Delta y \Delta z \tag{3.82}$$

$$\text{Output of A in } x \text{ direction} : \dot{m}_{Ax}|_{x+\Delta x} \Delta y \Delta z = \dot{m}_{Ax}|_x \Delta y \Delta z + \frac{\partial \dot{m}_{Ax}}{\partial x} \Delta x \Delta y \Delta z \tag{3.83}$$

$$\text{Rate of production of A by chemical reaction} : R'_A \Delta x \Delta y \Delta z \tag{3.84}$$

There are also output and input in other directions(y and z). After writing the entire mass balance and dividing by $\Delta x \Delta y \Delta z$ Eq. (3.85) is obtained.

$$\frac{\partial \rho_A}{\partial t} + \left(\frac{\partial \dot{m}_{Ax}}{\partial x} + \frac{\partial \dot{m}_{Ay}}{\partial y} + \frac{\partial \dot{m}_{Az}}{\partial z} \right) = R'_A \tag{3.85}$$

We can write the same input and output terms for component B. According to the law of conservation, it is valid to write:

$$R'_A + R'_B = 0 \tag{3.86}$$

$$\dot{m}_A + \dot{m}_B = \rho \cdot v \tag{3.87}$$

Equation (3.88) is called the equation of continuity and shows the total mass balance:

$$\frac{\partial \rho}{\partial t} + \nabla(\rho \cdot v) = 0 \tag{3.88}$$

Instead of writing balance equations in mass units, it is also possible to use molar units as below, where R_A is the molar rate of production of A per unit volume.

$$\frac{\partial C_A}{\partial t} + \left(\frac{\partial \dot{n}_{Ax}}{\partial x} + \frac{\partial \dot{n}_{Ay}}{\partial y} + \frac{\partial \dot{n}_{Az}}{\partial z} \right) = R_A \tag{3.89}$$

By substitution of Eq. (3.51) (Fick's first law) in $\dot{n}$, and under assumption of having no chemical reactions, the Fick's second law of diffusion is obtained:

$$\frac{\partial C_A}{\partial t} = D_{AB} \cdot \nabla^2 c_A \tag{3.90}$$

$$\text{with } \nabla^2 = \frac{\partial^2}{\partial x^2} + \frac{\partial^2}{\partial y^2} + \frac{\partial^2}{\partial z^2} \tag{3.91}$$

3.2.7.2 Heat Balance

The heat balance is, in principle, very similar to the mass balance. Using the general equation for the balance applied to a single burning particle as an example, leads to the following heat balance:

$$m \cdot c_p \cdot \frac{dT_2}{dt} = \alpha \cdot A(T_1 - T_2) + \varepsilon \cdot \sigma \cdot A\left(T_1^4 - T_2^4\right) + \Delta H_R(-r) \cdot V \quad \text{W or } \mathrm{Js}^{-1} \tag{3.92}$$

where

m mass of the particle in kg
T_2 particle temperature (assuming an isothermal particle) in K
c_p specific enthalpy of the particle in $\mathrm{J\,kg^{-1}\,K^{-1}}$
A surface area of the particle in $\mathrm{m^2}$

The term $\alpha \cdot A(T_1 - T_2)$ considers thermal conduction and convection and summarizes the input–output terms regarding this transport mechanism. $\varepsilon \cdot \sigma \cdot A \cdot \left(T_1^4 - T_2^4\right)$, is the thermal radiation including again input–output terms, and $\Delta H_R(-r) \cdot V$ is the heat generation term (source or sink term depending on the reaction enthalpy ΔH_R) by chemical reaction (combustion).

3.2.7.3 Momentum Balance

A momentum balance can be done for a finite volume leading, for a Newtonian and incompressible fluid, to the following Navier–Stokes equation with constant density.

$$\underbrace{\frac{\delta v}{\delta t} + (v\nabla)v}_{\text{acceleration}} = \underbrace{-\frac{1}{\rho}\nabla P}_{\text{pressure forces}} + \underbrace{v\Delta v}_{\text{viscous forces}} + \underbrace{g}_{\text{gravitational forces}} \tag{3.93}$$

The Navier–Stokes equations are very important in flow simulations.

3.3 Elementary Reactions and Radicals

3.3.1 Elementary Reactions

There are many ways of classifying a chemical reaction. One option is the distinction between homogeneous and heterogeneous reactions. A reaction is homogeneous if all reactants are located in the same phase where the reaction will take place, as is the case in combustion processes.

Chemical reactions can be written as global reactions or on an elementary chemical reaction basis, the correlation between stoichiometry and rate expression is important here.

The reaction between oxygen and hydrogen (old: Knallgas reaction) is a good example to explain the differences between global reaction (non-elementary) and the elementary reactions.

$$2H_2(g) + O_2(g) \rightarrow 2H_2O(g) \tag{3.94}$$

Reaction (3.94) shows the simple net reaction (global reaction) which consists of a multitude of reactions, like chain reactions, among others. The mechanism is complex and has not yet been fully elucidated. Some of the steps involve radicals, which are atoms or molecules with unpaired electrons. They are highly chemically reactive. A few elemental reactions of the hydrogen–oxygen reaction forming radicals are shown in the following:

$$\text{Initiation} \quad H_2 + O_2 \rightarrow H_2O + O^{\bullet} \tag{3.95}$$

$$\text{Propagation} \quad OH^{\bullet} + H_2 \rightarrow H^{\bullet} + H_2O \tag{3.96}$$

$$\text{Branching} \quad O_2 + H^{\bullet} \rightarrow OH^{\bullet} + O^{\bullet} \tag{3.97}$$

$$O^{\bullet} + H_2 \rightarrow OH^{\bullet} + H^{\bullet} \tag{3.98}$$

$$\text{Termination} \quad H^{\bullet} + H^{\bullet} + M \rightarrow H_2 + M \tag{3.99}$$

$$H^{\bullet} + O_2 + M \rightarrow HO_2^{\bullet} + M \tag{3.100}$$

A branching step is an elementary reaction which is characterized by the generation of more than one chain carrier, that is, a radical species. The third body (M) may be any stable species such as H_2, O_2, H_2O, N_2.

Compared to the rate laws of the elemental equations the rate of formation of radicals of the global reaction is complex, indicating a non-elementary reaction.

3.3.2 Reaction Rates

The rate of a reaction represents how fast a reaction takes place, for example, how fast product species are formed.

Consider the elemental chemical reversible reaction depicted as follows:

$$A + 2B \underset{k_{-1}}{\overset{k_1}{\rightleftarrows}} C + D \tag{3.101}$$

The net rate of reaction (3.101) is given by equation (3.102), or in general notation equation (3.104) for the general reaction (3.103)

$$r = k_1 C_A C_B^2 - k_{-1} C_C C_D \tag{3.102}$$

$$\nu_A A + \nu_B B \underset{k_{-1}}{\overset{k_1}{\rightleftarrows}} \nu_C C + \nu_D D \tag{3.103}$$

$$r = k_1 C_A^{\nu_A} C_B^{\nu_B} - k_{-1} C_C^{\nu_C} C_D^{\nu_D} \tag{3.104}$$

The reaction rate constants k_1 and k_{-1} refer to the forward reaction and reverse reaction, respectively. The rate law is a function of the reacting species and conditions like temperature, pressure, and concentrations of the species.

The correlation between reaction rate and concentrations is usually given in terms of power laws, which is exemplarily shown in Eq. (3.104). The exponents of the concentrations lead to the order of the reaction, whereas ν_A represents the order of the reaction with respect to reactant A, and ν_B the order with respect to reactant B. It is important to remember that the rate law expressions usually originate from experimental observations.

The rate of change of the amount of species i (R_i, in $\mathrm{mol\,s^{-1}\,m^{-3}}$) in j reactions is described in Eq. (3.105)

$$R_i = \sum_j \nu_{i,j} \cdot r_j \tag{3.105}$$

Where r_j is the specific reaction rate of a reaction j and is expressed in Eq. (3.106).

$$r_j = \underbrace{\frac{\mathrm{d}N_i}{\mathrm{d}t} \cdot \frac{1}{V}}_{R_i} \cdot \frac{1}{\nu_i} \tag{3.106}$$

3.3.3 Temperature Dependence

The temperature dependence of chemical reactions is usually described by the Arrhenius equation.

$$k_i = k_{0,i} \cdot e^{-\frac{E_i}{R \cdot T}} \tag{3.107}$$

Where $k_{0,i}$ represents the so-called frequency factor, R is the universal gas constant, and E_i is the activation energy of the reaction in J mol^{-1}.

In addition, and when necessary, an extended Arrhenius equation is used, usually in gas-phase chemistry. In this equation three parameters are applied to describe the temperature dependence:

$$k_i = \underbrace{k_{0,i} \cdot T^{\eta_i}}_{k_{i,1}} \cdot \underbrace{e^{-\frac{E_i}{R \cdot T}}}_{k_{i,2}} \tag{3.108}$$

The coefficient $k_{i,1}$ represents the frequency of collision and is a function of temperature only. In case of $\eta_i = 0$, the extended Arrhenius approach turns into the basic Arrhenius approach, the case of $\eta_i = 1/2$ is derived from the collision theory for bimolecular reactions, and $\eta_i = 1$ derives from activated complex or transition state theory.

The Arrhenius equation is used to determine the activation energy by measuring the rate of reaction at different temperatures. By linearizing the Arrhenius law a plot of $\ln(k_i)$ as function of $(1/T)$, called an Arrhenius plot (Figure 3.17), is formed as follows:

$$\ln(k_i) = \ln(k_{0,i}) - \frac{E}{R}\left(\frac{1}{T}\right) \tag{3.109}$$

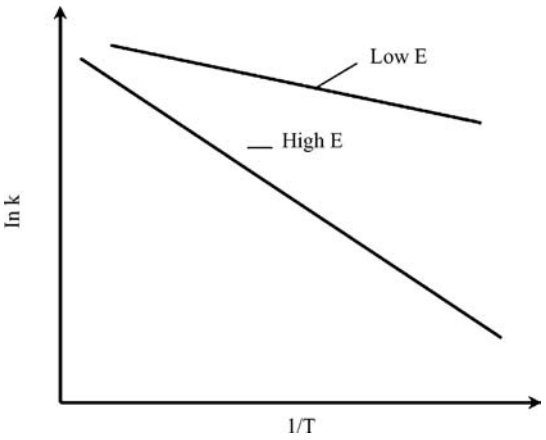

Figure 3.17 Temperature dependence of the reaction rate – Arrhenius plot.

In the Arrhenius plot the slope depicts the ratio $-E/R$, where a large slope characterizes a large activation energy and a small slope indicates a small activation energy.

3.3.4 Collision Theory

The Arrhenius' law is similar to the results of the collision theory, which says that reactants first have to physically meet in order to take part in a chemical reaction. Next, they have to collide with a certain energy, called the activation energy, which is high enough that the reaction can take place.

The average kinetic energy of a substance is proportional to its thermodynamic temperature, which in turn is proportional to the square of its speed. The consequences of this higher speed at higher temperatures are more frequent collisions, and the collisions are more energetic. The kinetic theory of gases leads to the collision rate of molecules in a gas. If bimolecular (molecules A and B) collisions are considered, the number of collisions of A with A per time (s) and volume (cm^3) (Z_{AA}) are calculated via equation (3.110). Collisions of molecule A with B per s per $cm^3 Z_{AB}$ are calculated via equation (3.111). These equations calculate the rate equations of bimolecular reactions, provided every collision between a reactant molecule results in the conversion of reactants into product.

$$Z_{AA} = d_A^2 \underbrace{\frac{\mathcal{N}^2}{10^6} C_A^2}_{n_A} \sqrt{\frac{4\pi kT}{M_A}} \tag{3.110}$$

$$Z_{AB} = \left(\frac{d_A + d_B}{2}\right)^2 n_A n_B \sqrt{8\pi kT\left(\frac{1}{M_A} + \frac{1}{M_B}\right)} \tag{3.111}$$

Z_{AA}	number of collisions of A with A ($s^{-1}\,cm^{-3}$)
Z_{AB}	number of collisions of A with B ($s^{-1}\,cm^{-3}$)
d_A	diameter of an A molecule (cm)
d_B	diameter of a B molecule (cm)
$\mathcal{N}$	Avogadros's number $= 6.023 \times 10^{23}\,mol^{-1}$
C_A	concentration of A ($mol\,l^{-1}$)
C_B	concentration of B ($mol\,l^{-1}$)
n_A	$\mathcal{N} \cdot C_A/10^3$ number of molecules of A per cm^3
n_B	$\mathcal{N} \cdot C_B/10^3$ number of molecules of B per cm^3
k	Boltzmann constant $= 1.30 \times 10^{-16}\,erg\,K^{-1}$
T	Temperature (K)
M_A	molecular mass/$\mathcal{N}$ = mass of an A molecule (g)
M_B	molecular mass/$\mathcal{N}$ = mass of a B molecule (g)

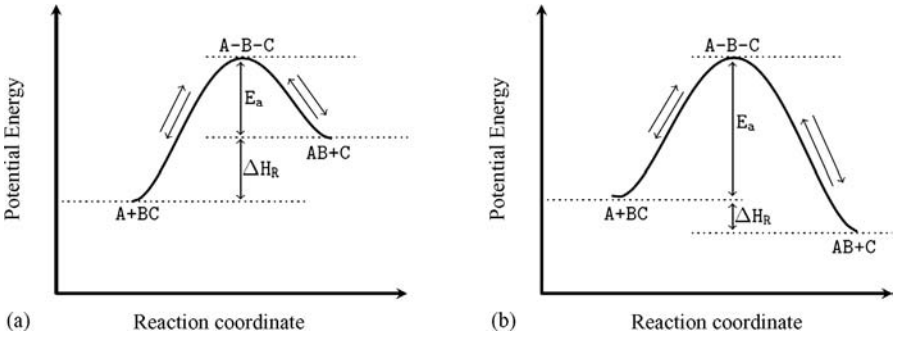

Figure 3.18 Comparison of an endothermic reaction (a) and an exothermic reaction (b).

As mentioned before, the molecules have to collide with a certain minimum energy, the activation energy. The activation energy can be visualized as a barrier to the energy transfer between reacting molecules. For the reaction (3.112) the energies involved in transformation of the reactants to products are depicted in Figure 3.18 when the reaction is endothermic (a) and exothermic (b).

$$A + BC \rightleftarrows A-B-C \rightleftarrows AB + C \tag{3.112}$$

Figure 3.18 shows the potential energy of the three molecule system A, B, C and the reaction progress. The chemical potential energy describes the energy of a species with regards to the arrangement of the atoms. The bonds between the atoms are a source of potential energy.

First the reactants A and BC are far apart. The system's energy at that point is just the bond energy of BC. By moving along the reaction coordinate, the reactants approach each other and the BC bond energy begins to break. At this point the energy of the system increases. At the maximum, intermolecular distances between A and B and between B and C are equal (A-B-C), which causes the high potential energy of this state. At the end of the reaction, the molecules A and B approach each other while decreasing the potential energy of the system by using it as bond energy, and C is far apart, refer also to [2].

3.3.5
Three-Body Reactions

Sometimes third bodies are required so that reactions can proceed. This body, called M, has to appear in the rate expression. Some third body species work better than others.

Some radical recombination reactions do not fulfill the Arrhenius approach. The energy, which is released by recombination of two radicals, is so large that it causes the product to decompose into its original radicals. Therefore, a third body is necessary to bind this energy so that the recombination can

continue. Considering the chemical reaction (3.113), the rate law is given by Eq. (3.114).

$$H^{\bullet} + H^{\bullet} + M \underset{k_{-1}}{\overset{k_1}{\rightleftharpoons}} H_2 + M \tag{3.113}$$

$$r = k_1 C_{H^{\bullet}}^2 C_M - k_{-1} C_{H_2} C_M \tag{3.114}$$

Most three-body recombination reactions are pressure-sensitive. This means, that they occur at high pressure and rarely at low pressure.

3.3.6
Chemical Equilibrium

The chemical equilibrium is dynamic in nature where no net flows of species or energy appear.

The forward and reverse reaction rates of the elementary reaction are given in Eq. (3.115).

At equilibrium this equation can be combined to give the chemical equilibrium constant (K_c):

$$\frac{k_1}{k_{-1}} = K_C = \frac{C_C^{\nu_C} C_D^{\nu_D}}{C_A^{\nu_A} C_B^{\nu_B}} \tag{3.115}$$

3.3.7
Gibbs Enthalpy

In order to describe the chemical equilibrium from the thermodynamic aspect, the Gibbs energy (Δg^0) is introduced and applied to the chemical reaction as follows:

$$\Delta g^0 = \Delta h^0 - T \cdot \Delta s^0 \tag{3.116}$$

Δg^0 standard molar Gibbs enthalpy of reaction ($J\,mol^{-1}$)
Δh^0 standard molar enthalpy of reaction ($J\,mol^{-1}$)
T temperature (K)
Δs^0 standard molar entropy of reaction ($J\,mol^{-1}\,K^{-1}$)

At constant pressure and temperature a correlation between the Gibbs enthalpy (Δg^0) and the dimensionless equilibrium constant (K_c') can be derived from thermodynamic fundamental equations.

$$K_C' = e^{(-\Delta g^0/(R.T))} \tag{3.117}$$

R ideal gas constant = $8.314\,J\,mol^{-1}\,K^{-1}$
K_C' dimensionless equilibrium constant

So if all the enthalpies of the species (h_i^0) are known as well as all the entropies (s_i^0) at the given conditions, the enthalpy difference and entropy difference can be calculated as follows:

$$\Delta h^0 = \sum \nu_i \cdot h_i^0 \tag{3.118}$$

$$\Delta s^0 = \sum \nu_i \cdot s_i^0 \tag{3.119}$$

then Δg^0 can be calculated and hence K_c'. Knowing K_c' and the stochiometric coefficients (ν_i) K_c is usually obtained using the thermodynamic properties in pressure units as follows:

$$K_c = K_c' \cdot (P_{ref}/(R \cdot T))^{\Sigma \nu_i} \tag{3.120}$$

P_{ref} is the reference pressure (usually 1 atm).

3.3.8 Radicals

In order to understand what a radical is, it is important to know about the chemical bonds between the atoms. They consist of pairs of electrons, which are shared by two atoms. The chemical bond can be seen as the attraction between atoms, and the bond-dissociation energy is the measure of the strength of a chemical bond. The energetic state of a molecule is lower than the energy state of the molecule dissociated into its atoms. In order to split the two shared electrons of the bond by homolysis, sufficient energy amounts have to be supplied. The minimum energy amount involved has to be the bond-dissociation energy. In this way extremely reactive species, called radicals, are produced.

There are two ways to cleave a molecule (X–Y) into its atoms. By distributing the electrons unequally, the more electronegative part accepts electrons as the less electronegative part loses electrons. The cleavage results in two ions, X^+ and Y^-. This process is termed heterolytic cleavage or heterolysis (reaction (3.121)). The energy involved is called the heterolytic bond-dissociation energy.

$$X - Y \Rightarrow X^+ + Y^- \tag{3.121}$$

In comparison, the two electrons of one single bond can distinguish evenly. This process is termed homolytic cleavage or homolysis (reaction (3.122)) and generates high energy carrying species, called radicals ($X^\bullet$,$Y^\bullet$).

$$X - Y \Rightarrow X^\bullet + Y^\bullet \tag{3.122}$$

In general, radicals are an extremely reactive species, reacting rapidly with the majority of molecules. All radical initiation processes require sufficient amounts of energy which can be supplied by thermolysis, photolysis, or ionizing radiation (e.g., X-rays).

Some of the main reactions of radicals are listed in the following:

$$XY \Rightarrow X^{\bullet} + Y^{\bullet} \quad \text{Initiation} \tag{3.123}$$

$$X^{\bullet} + Y^{\bullet} \Rightarrow XY \quad \text{Combination} \tag{3.124}$$

$$X^{\bullet} + YZV^{\bullet} \Rightarrow XY + ZV \quad \text{Disproportionation} \tag{3.125}$$

$$XY^{\bullet} \Rightarrow X^{\bullet} + Y \quad \text{Fragmentation} \tag{3.126}$$

$$X^{\bullet} + YZ \Rightarrow XY + Z^{\bullet} \quad \text{Radical transfer} \tag{3.127}$$

$$X^{\bullet} + YZ \Rightarrow XYZ^{\bullet} \quad \text{Addition} \tag{3.128}$$

Radicals mostly exist as transient intermediates and never occur in high concentrations. That is the reason why radical transfer and addition is predominant causing chain reactions.

3.3.9
Development and Analysis of a Set of Reactions

In general, a chemical reaction consists of a sequence of many elementary reactions which defines the reaction mechanism of the net reaction. Especially in combustion, the number of elementary reactions can increase to several thousands.

As an example the complex reaction path of fuel-nitrogen to NO, N_2O and N_2 is depicted in Figure 3.19. It gives a general overview and shows the most important reaction routes. Another scheme is given in Figure 3.20 for methane oxidation. From such general reaction routes a simplified set of chemical reactions is developed, as given in Table 3.3 summarizing NO formation from fuel-nitrogen.

Complex reaction mechanisms can be analyzed with regard to the species flow (reaction flow analysis) showing the main reaction routes. Another method is sensitivity analysis showing the most sensitive reactions for the determination of the final product. Sensitivity coefficients are defined as follows:

$$S = \mathrm{d}P/\mathrm{d}K \tag{3.129}$$

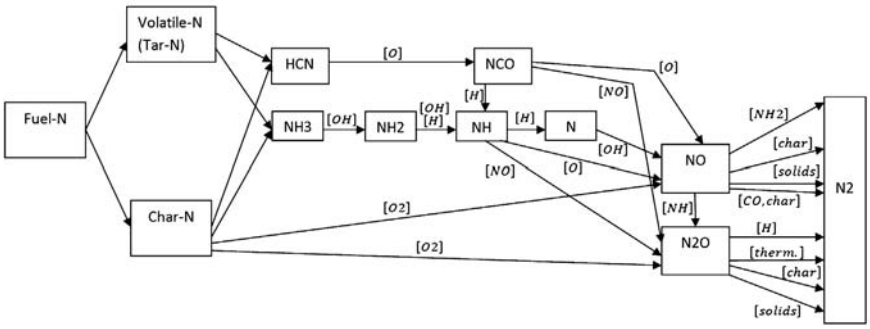

Figure 3.19 A complex set of reactions leading to NO_x from fuel nitrogen.

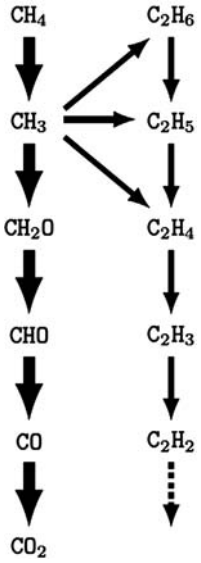

Figure 3.20 The main oxidation routes for methane combustion. The arrows indicate the most important routes. The width of the arrows corresponds to the species relative flow under the given conditions.

Table 3.3 A simplified fuel nitrogen conversion mechanism.

Used Reactions

No.				Catalyst
1	$NCO + O$	$\rightarrow$	$NO + CO$	
2	$NCO + OH$	$\leftrightarrow$	$NO + CO + H$	
3	$NH + O$	$\leftrightarrow$	$NO + H$	
4	$NCO + NO$	$\leftrightarrow$	$N_2O + CO$	
5	$NH + NO$	$\leftrightarrow$	$N_2O + H$	
6	$NH_2 + NO$	$\rightarrow$	$N_2 + H_2O$	
7	$N_2O + CO$	$\leftrightarrow$	$N_2 + CO_2$	
8	$N_2O + H$	$\leftrightarrow$	$N_2 + OH$	
9	$N_2O + OH$	$\leftrightarrow$	$N_2 + HO_2$	
10	$N_2O + O$	$\leftrightarrow$	$2\ NO$	
11	$N_2O + O$	$\leftrightarrow$	$N_2 + O_2$	
12	$N_2O + M$	$\leftrightarrow$	$N_2 + O + M$	
13	$HCN + O$	$\leftrightarrow$	$NCO + H$	
14	$NH_3 + O$	$\leftrightarrow$	$NH_2 + OH$	
15	$NH_2 + O$	$\leftrightarrow$	$NH + OH$	
16	$NO + CO$	$\rightarrow$	$1/2\ N_2 + CO_2$	bed mat.
17	$NO + 2/3\ NH_3$	$\rightarrow$	$5/6\ N_2 + H_2O$	bed mat.
18	$NH_3 + 3/4\ O_2$	$\rightarrow$	$1/2\ N_2 + 3/2\ H_2O$	bed mat.
19	NH_3	$\rightarrow$	$1/2\ N_2 + 3/2\ H_2$	bed mat.
20	$N_2O + CO$	$\rightarrow$	$N_2 + CO_2$	bed mat.

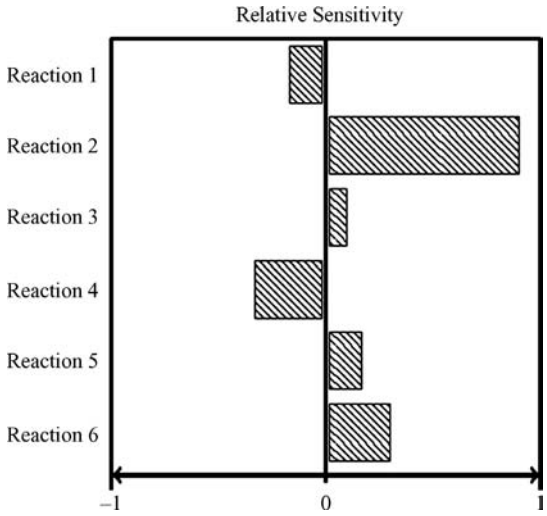

Figure 3.21 Sensitivity analysis of a set of reactions showing that reaction 2 is of high importance for the result because of its high sensitivity.

S sensitivity or sensitivity coefficient (units depend on the parameters used)
P any parameter, for example, concentration of a certain species C_i (mol m^{-3})
K any parameter, for example, rate constant (s^{-1})

Because of the difficulty with different units dimensionless sensitivity coefficients (or relative sensitivity coefficients, S_{rel}) are defined. They are based on standard parameters (here P_0, K_0) for example, initial concentrations.

$$S_{rel} = (dP/P_0) \cdot (K_0/dK) \tag{3.130}$$

Sensitivity analysis is a powerful tool, increasing the understanding of the mechanism and its most sensitive parameters. Figure 3.21 shows a typical result of a sensitivity analysis. It reveals that the kinetic data for reaction 2 is very important for the final result. Therefore the kinetic data of reaction 2 should be well known.

3.3.10
Simplification of a Set of Reactions

Complex reaction sets usually lead to a stiff set of differential equations which are numerically difficult to solve. Two frequently used methods of simplification of reaction sets are the steady-state approximation and the partial equilibria. The approach of partial equilibria originates from the assumption of fast forward and reverse reactions. This simplification applies especially at high temperatures.

3.4
Ignition

3.4.1
Introduction

As mentioned earlier in this book, combustion is a ubiquitous technology. It accounts for approximately 85% of global primary energy production. *Ignition* is the process of starting combustion. It influences the quality of combustion, that is, speed, pollutant formation, probability of flame formation, and others [1]. In technical applications, such as in engines, reliable ignition that prevents misfiring is important, whereas the prevention of undesired ignition is critical for safety reasons in the process industries and other sectors [2,3]. This chapter presents the fundamentals of ignition (auto-ignition and induced ignition), plus some information on desired ignition processes including alternative technologies for ignition. Chapter 7 treats the prevention of undesired ignition.

3.4.2
Autoignition

Autoignition is the onset of a combustion process without support by an external ignition source. Since the autoignition temperature (AIT) depends on several parameters, such as fuel, stoichiometry, pressure, reaction volume and reaction vessel, precise conditions are necessary for its determination. AIT can be defined as follows: "*The autoignition temperature of flammable gases or liquids is the lowest wall-temperature measured in a glass flask by a method prescribed for its determination, at which the developing inhomogeneous gas/air or vapor/air mixture will just be stimulated to burn as a flame*" (see DIN 51794 and IEC 60079-4). A synonymous expression for the AIT is "*minimum ignition temperature*".

The dependence of the autoignition temperature on the vessel size and vessel walls is related to heterogeneous chain termination reactions (quenching, see also mechanism of combustion, "radical chain reactions"). For gases, AIT is easiest to define. For liquids, AIT depends on the droplet size. The autoignition temperature of mists can be lower than the flash point of their respective liquid, caused, for example, by decomposition reactions.

At stoichiometric conditions and at high pressures, autoignition is favored. In oxygen, it may occur at temperatures up to 300 °C below that in air. Table 3.4 presents a few examples of autoignition temperatures in gases (all at stoichiometric mixing ratio and standard pressure), reprinted with permission from [4].

Auto-ignition is encountered in the following cases:

- Diesel engine (heating of the gas in the cylinders by compression prior to fuel injection)
- Fresh humid, decaying haystack (heat is confined and increases till ignition)

Table 3.4 Minimum ignition temperatures of common fuels. (Source: [4].

Fuel		Minimum Ignition Temperature (°C)	
		in air	in O_2
Butane	C_4H_{10}	405	283
Carbon monoxide	CO	609	588
Ethane	C_2H_6	472	
Hydrogen	H_2	572	560
Methane	CH_4	632	556
Propane	C_3H_8	493	468

Autoignition can occur with gaseous, liquid and solid fuels, and it can be intentional or unintentional.

3.4.3 Induced Ignition

In induced ignition, an ignition source is used to start combustion. Ignition sources can be hot surfaces, sparks, flames and others. The ignition source can be activated on purpose, such as in an Otto engine, or it can be caused unintentionally, for example, an electrostatic discharge. In contrast to autoignition, induced ignition of gases does not require a minimum temperature.

For liquids, there are two temperatures of interest: *flash point* and *fire point*.

By definition, the *flash point* is the lowest temperature at which the vapor formed above a pool of the liquid can be ignited in air at a pressure of 1 atmosphere under specified test conditions. The "closed cup" and the "open cup" method are used. Small impurities of low-boiling flammable liquids or gases will lower the flash point, and the flash point of a mixture may be lower than that of the individual components. The flash point measured in a closed cup is used for the classification of flammable liquids in important regulations such as GefStoffVO, VbF, ADR, RID, IMDG Code, UN Recommendations and IATA code. At the flash point, the flame will stop as soon as the ignition source is removed. By contrast, the *fire point* is the lowest temperature at which the sample will support combustion for at least 5 s. Above the fire point, the temperature is high enough to keep the flame alive with freshly formed vapors. Hence, the fire point is always a few degrees above the flash point. The fire point depends on the vapor pressure of the respective substances. Figure 3.22 shows a lab experiment to check the flash point of a liquid.

In Table 3.5 data for gasoline and diesel are provided to illustrate the difference between flash point (induced ignition) and autoignition temperature. For details, the following norms can be consulted: ASTM D93, IP34, ISO 2719, DIN 51758, JIS K2265 and EN ISO 3679.

Although the flash points of diesel and gasoline differ significantly, the autoignition temperatures are close to each other.

Figure 3.22 This liquid is too cold, the flash point is not reached.

Table 3.5 Comparison of flash point and autoignition temperature.

	Flash Point (°C)	Autoignition Temperature (°C)
Gasoline	−20	240
Diesel	55	220

The spread between flash point and fire point depends on the volatility (vapor pressure) of the fuel. As shown in Table 3.6 for two examples, a higher flash point will usually give a higher delta to the fire point, too. The fire point is always above the flash point.

Liquid fuels are often burned as *sprays*. In this mode, one can distinguish between three autoignition processes: droplet ignition, group ignition and spray ignition [5], see Figure 3.23.

For solid fuels, typical autoignition temperatures are provided in Table 3.7.

Important to note is that the autoignition temperature of decomposition products from solids often lies significantly below that of the solids themselves. A good example is a pile of wet grass. Due to the confinement, the heat production results in a runaway reaction where self-heating finally ignites the decomposition products of the hay.

Dusts are characterized by a high surface/volume ratio. Therefore, fine dusts, typically $< 100\,\mu m$, when suspended in air, can be ignited easily, as opposed to large chunks of the same solids, see also Chapter 7. Hybrid mixtures, that is, compositions that contain two phases, tend to ignite more easily than the pure constituents.

Table 3.6 Flash point and fire point for two liquid hydrocarbons.

Substance	Flash Point (°C)	Fire Point (°C)	Difference (°C)
Benzene	−11	−9	2
Lubrication oil	148	190	42

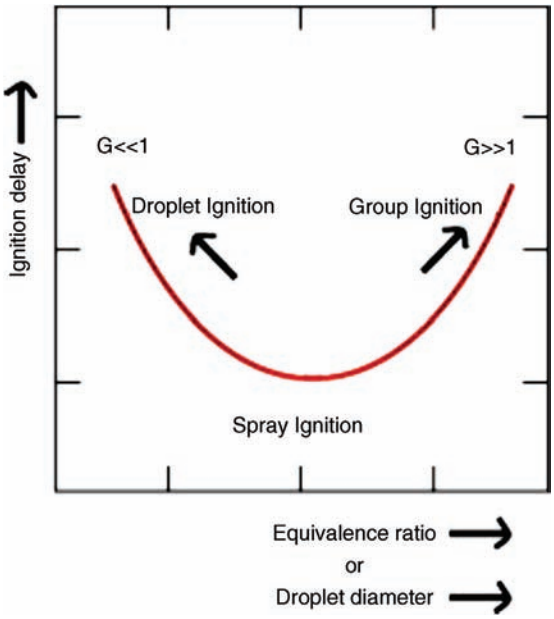

Figure 3.23 Qualitative description of the three autoignition modes in sprays. Reproduced from [5].

Table 3.7 Autoignition temperature of solids.

Material	Autoignition Temperature (°C)
White phosphorus	60
Newspaper	240
Cotton wool	260
Hardwood	295
PVC	530

3.4.4 Theoretical Models for Ignition

There are two commonly used models for ignition:

- Theory of *Semenov* (homogeneous ignition, thermal explosion)
  It is useable as long as there is no temperature gradient. An example for a thermal explosion is the reaction: $Cl_2 + H_2$
- Theory of *Frank-Kamenetskii* (inhomogeneous ignition)
  This model allows a temperature gradient to be taken into account, which occurs when there is a high resistance to heat transfer in the reacting system, or when the system has reactants with a low thermal conductivity and/or highly conducting walls.

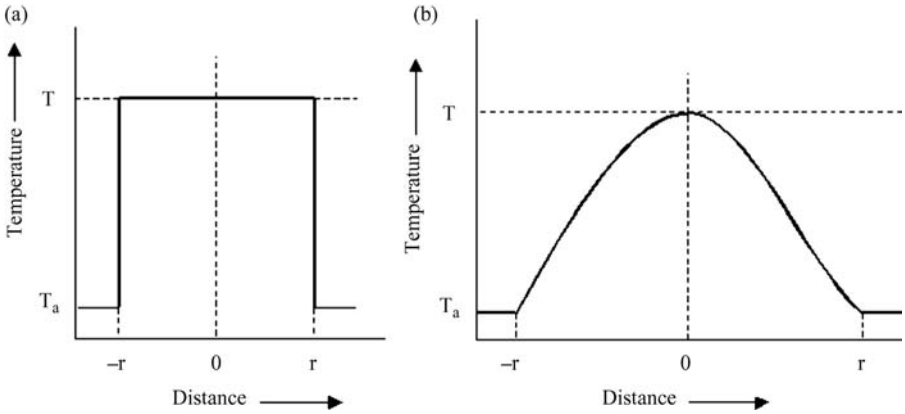

Figure 3.24 Temperature profiles in the models of Semenov (a) and Frank–Kamenetskii (b).

The temperature profiles for the two models are shown schematically in Figure 3.24.

Details can be found in [6].

3.4.5 Explosives

Explosives [7] are characterized by a very fast oxidation reaction. They detonate rather than burn by consuming oxygen within the compound rather than from the ambient air, and the expansion of the hot evolving gases gives off energy. Explosives can be grouped into two basic categories: low explosives and high explosives. The former tend to deflagrate, the latter to detonate. Low explosives are used in fire arms and space rockets. Black powder (gun powder) was a very common low explosive that is still used in fireworks. However, it is quite unsafe and has, therefore been widely replaced. The first high explosive used for commercial blasting operations was nitroglycerine, also called "blasting oil." Nitroglycerine is an unstable chemical and therefore dangerous to use. This was improved when Alfred Nobel invented dynamite by mixing nitroglycerine with kieselguhr. Today, explosives are used in mining, building demolition, pyrotechnics, and construction. They also inflate airbags and activate seatbelt pretensioners.

Homogeneous, that is, one-component explosives, have unstable chemical structures that contain O—O bonds (peroxides) or $-N_3$ (azides), for instance. The structure of trinitrotuluene (TNT) is shown in Figure 3.25.

An important value of explosive materials such as liquid peroxides is the SADT (self-accelerating auto decomposition temperature), a term that is self-explanatory and important for storage and transportation. At 10 K below the SADT, one speaks about the "emergency temperature".

So-called *hypergolic mixtures* react spontaneously upon contact of the two reaction partners. They will produce reliable ignition and hence are used, for example, in

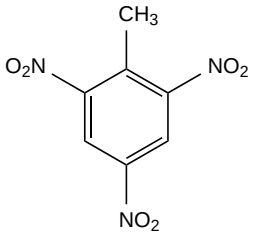

Figure 3.25 Formula of the explosive TNT (2,4,6-trinitrotoluene). Upon detonation, TNT decomposes according to $2\,C_7H_5N_3O_6 \rightarrow 3\,N_2 + 5\,H_2 + 12\,CO + 2\,C$. The reaction is exothermic but has a high activation energy.

rockets. An example of such a mixture is derivatives of hydrazine with N_2O_4, for example, UDMH (2-dimethylhydrazine).

3.4.6 Flammability Limits

The range in which a mixture of fuel and oxidizer will ignite is called the flammability range, flanked by lower and upper flammability limits (synonymous: explosive limits, ignition limits). Typically, they are given as vol%, see Table 3.8.

One can see from this table that hydrogen has a very wide flammability range. Its danger upon accidental release, however, is significantly reduced because it will diffuse very fast, as opposed to, for example, propane and butane, which are heavier than air (This is why LPG-powered cars are forbidden in some underground parking areas; LPG, liquefied petroleum gas, is a mixture of propane and butane, which can be liquefied at room temperature under pressure). In oxygen, all gases have wider flammability ranges than in air or in dilution with another inert gas. Outside the flammability limits, a gaseous fuel/oxidizer mixture is too "fat" or too "lean" for ignition.

Table 3.8 Flammability limits of common fuels at standard temperature and pressure. (Source: [4].)

Fuel		Flammability Limits (% of fuel gas by volume)			
		in Air		in O_2	
		Lower	Upper	Lower	Upper
Butane	C_4H_{10}	1.86	8.41	1.8	49
Carbon monoxide	CO	12.5	74.2	19	94
Ethane	C_2H_6	3.0	12.5	3	66
Hydrogen	H_2	4.0	74.2	4	94
Methane	CH_4	5.0	15.0	5.1	61
Propane	C_3H_8	2.1	10.1	2.3	55
Propylene	C_3H_6	2–4	10.3	2.1	53

Note: Flammability limits can be given by volume or by mass (conversion possible via density). For dusts, only the lower flammability limit is of practical interest.

The flammability limits depend on the pressure of the mixture. For mixtures of several gases, the flammability limits can be estimated with the *Rule of Le Chatelier*:

$$IL_{\text{mixture}} = \frac{1}{x_1 \cdot \left(\frac{1}{IL_1}\right) + x_2 \cdot \left(\frac{1}{IL_2}\right) + x_3 \cdot \left(\frac{1}{IL_3}\right) + \ldots + x_n \cdot \left(\frac{1}{IL_n}\right)} \tag{3.131}$$

where IL_i stands for the "ignition limit", x_i for the mole fraction and $i = 1, 2, 3, \ldots n$ for the number of gas species. The rule of Le Chatelier provides a fairly good estimation (exception: acetylene/air).

Here is an example:

The upper ignition limit of C_3H_8 is 10.1%, and for H_2 it is 74.2%. Therefore, the upper explosive limit of a mixture that contains 40% propane and 60% hydrogen can be estimated to be 21%:

$$UL_{\text{mixture}} = \frac{1}{0.4 \cdot \left(\frac{1}{10.1}\right) + 0.6 \cdot \left(\frac{1}{74.2}\right)} = 21.0\%$$

3.4.7 Minimum Ignition Energy

The minimum ignition energy (MIE) of flammable gases, vapors or dust clouds is defined as the minimum value of the electric energy, capacitively stored in a discharge circuit which – upon discharge across a spark gap – ignites the standing mixture in the most ignitable composition (see ASTM E582-76). MIE is given in mJ. Typical values of MIE are 10^{-3} to 10^{-1} mJ for explosives, hydrogen and hydrocarbons in oxygen. (Figure 3.26) Static electricity is on this level and can hence cause an ignition of several gas/air mixtures. Typical dust/air mixtures can be ignited between 1 mJ and 1–10 J, that is, only with much higher energies. The finer a dust is, the easier it will be to ignite.

Compare with flammability limits: As they are approached, MIE increases sharply. The lowest value of MIE is around the stoichiometric mixture. The heavier a fuel becomes, the more MIE will move into the fuel-rich area as larger molecules are diffusing to the ignition spot more slowly.

3.4.8 Quenching and Maximum Experimental Safe Gap (MESG)

The term "*quenching*" denotes the sudden inactivation of radicals. When radicals, which are necessary for sustaining a combustion reaction, reach a (cold) surface like a vessel wall, they react and are no longer available. This is then a heterogeneous chain termination process, as opposed to a "homogeneous chain termination" reaction which can occur in the gas phase as a three-body collision. Quenching leads

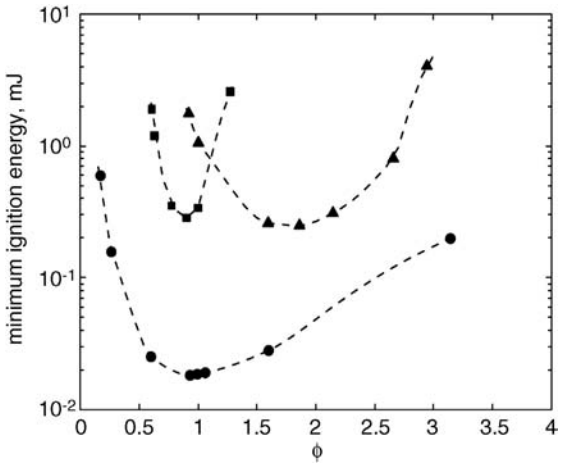

Figure 3.26 Minimum ignition energies of (●) hydrogen/air, (■) methane/air and (▲) heptane/air mixtures in relation to ϕ (the equivalence ratio) at atmospheric pressure. Reproduced with permission from [8].

to soot and CO formation in internal combustion engines, but it can also be used for safety purposes, as is illustrated by Davy's lamp (see Figure 3.27). In this device, a fine grid of metal prevents a flame inside from igniting potentially explosive gases on the outside.

Davy's lamp was used in coal mines where methane that had desorbed from the coal seams led to several catastrophic explosions in the past. It brought a tremendous

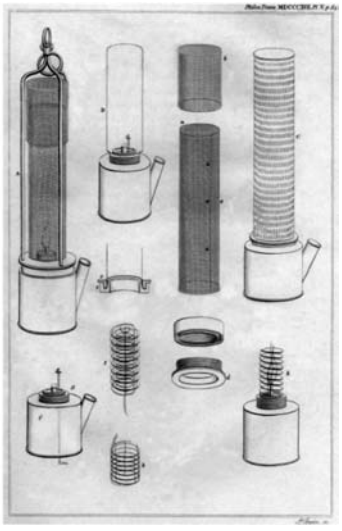

Figure 3.27 Davy's miners' lamp. Source: [9].

gain for miners' safety. An important term in this context is the so-called *maximum experimental safe gap* (MESG). A fine wire mesh in a tube filled with a combustible fuel/air mixture will not let a flame pass through below a certain minimum wire-to-wire distance (the MESG), the reason being flame quenching: the metal wires extract heat and quench the radicals at their surface.

MSEG depends on the gas. Note that turbulent explosions can be transmitted through openings smaller than the laminar flame quenching distance! The norm on MESG is IEC 60079. MESG is an important safety parameter in process engineering. It is used to design flame arrestors.

3.4.9
*p*T Explosion Diagram

The so-called *pT* explosion diagram (*p* stands for pressure and *T* for temperature) is very instructive to understand ignition. It is depicted in Figure 3.28 for the O_2/H_2 system. One can see an S-shaped curve over the temperature versus pressure chart.

To understand the *pT* explosion diagram, let us pick the following point in Figure 3.28: 800 K, 1.3 mbar (523 °C, 1 mm Hg) – there is no explosion. Instead, O_2 and H_2 only react slowly with each other, resulting in a gradual mixture consumption, temperature increase and water formation.

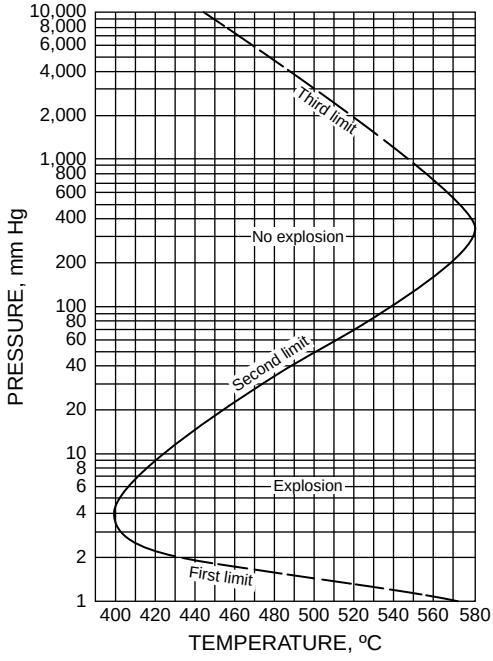

Figure 3.28 *pT* explosion diagram for H_2 in oxygen. Test conditions: stoichiometric mixture, spherical vessel with volume 7.4 cm^3 coated with KCl. Reproduced with permission from [6].

Under these conditions, radicals diffuse to the vessel walls where they are quenched. According to Fick's law, the diffusion coefficient is inversely proportional to pressure, so the low pressure of 5 mbar lets the radicals dissipate away.

$$\text{Fick's law}: J = D^{*}\delta c/\delta t \tag{3.132}$$

with J being the mass flow in $\mathrm{mol\,m^{-2}\ s^{-1}}$, D the diffusion coefficient, c the concentration and t the time. As the diffusion coefficient is inversely proportional to pressure ($D \sim 1/p$), diffusion will be more important at low pressures as in the above-described situation at 5 mbar.

Let us now proceed in the diagram to higher pressures, for example, 800 K and 50 mbar (37.5 mm Hg): one observes that above approximately 2 mbar, the mixture will explode. Explanation: After passing the so-called "first explosion limit", diffusion cannot keep pace with the formation of radicals in the gas phase, and spontaneous ignition occurs. Since there is a competition between chain branching (radical formation) and radical quenching, the properties of the vessel wall show a strong influence in this first explosion limit.

Let us further increase the pressure to >150 mbar (112.5 mm Hg), 800 K: again there is no ignition as the "second ignition limit" is passed. In this region, the competition between chain branching reactions and chain termination reactions is dominant.

At low pressures, the following reaction is favored : $H^{\bullet} + O_2 \rightarrow OH^{\bullet} + O^{\bullet}$
At higher pressures, this reaction gains importance : $H^{\bullet} + O_2 + M \rightarrow HO_2{}^{\bullet} + M$

M is a third gas molecule (quenching partner).

$HO_2^{\bullet}$ exhibits a much lower reactivity than $OH^{\bullet}$, hence this reaction corresponds essentially to chain termination. Three-body-collisions are favored at high pressures. The third body is necessary to carry away the recombination energy in homogeneous reactions, whereas the reaction wall plays this role in heterogeneous reactions.

Now as the pressure is further increased on our journey through Figure 3.28, one reaches the "third explosion limit" and the realm of "thermal ignition". In this region, there is a competition between heat generation ($\sim x^3$) and heat dissipation ($\sim x^2$).

Note: For hydrocarbons, the pT explosion diagram is more complex. There are, around the third ignition limit, zones of "cool flames" and multi-stage ignition.

Explanation of *cool flames*:

A cool flame is one that burns at about a maximum temperature of 120–600 °C, which is significantly below ordinary combustion temperatures. A typical temperature increase upon ignition of a cool flame is a few 10 °C only. Cool flames are responsible for engine knock with low octane-grade fuels in internal combustion engines. A cool flame is a faint, luminous combustion that proceeds slowly and with little heat emission under incomplete combustion. The phenomenon was first observed by Sir Humphry Davy in 1817, who discovered that he did not burn his fingers and could not ignite a match in a cool flame. A cool flame reaction never proceeds to complete combustion. Instead, fuel and oxidizer break down and recombine to a variety of stable chemical compounds, including alcohols, acids,

peroxides, aldehydes, and carbon monoxide. Cool flames have an oscillating character and can sustain for a long period of time.

In engines, cool flames are associated with two-stage-ignition and characterized by an NTC (negative temperature coefficient). Whereas in normal reactions, the reaction rate increases with temperature, the opposite is observed under some engine conditions. *Degenerate branching* is a chain termination process as the temperature is increased: the precursor substances are thermally unstable, therefore, they are inactivated and the chain branching reaction is deprived of its foundation. More details on cool flames can be found in [10], images in [11].

3.4.10
Ignition Delay Time

When an explosive gas/air mixture is ignited, the pressure rise is not noticed immediately. Instead, a certain time, the so-called ignition delay time, has to elapse. In this time, the radical pool is being built up. In the beginning, the flame kernel is still very small. As it grows, it consumes more and more combustible material and finally produces a noticeable signal. The definition of onset or start of combustion is arbitrary. Typical definitions are 5% of maximum pressure reached or 2% of fuel consumed, and so on.

The ignition delay time can be considered an induction time. Figure 3.29 provides an example.

The ignition delay time depends on the temperature as follows: $\tau = Ae^{\frac{B}{T}}$, see Figure 3.30. A is the pre-exponential factor, B another constant, and T the temperature.

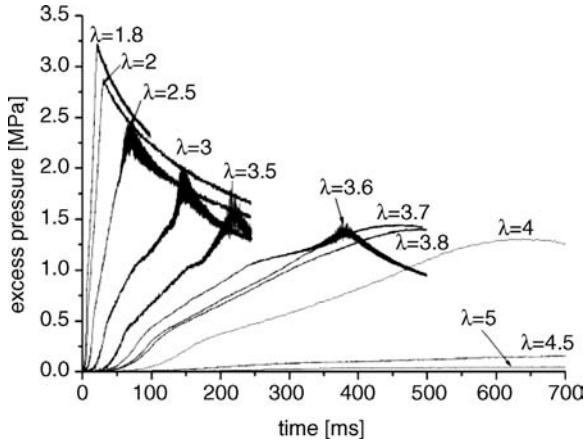

Figure 3.29 Ignition delay time of various hydrogen/air mixtures in a closed reaction vessel. One can see that the leaner the mixture, the longer the ignition delay time.

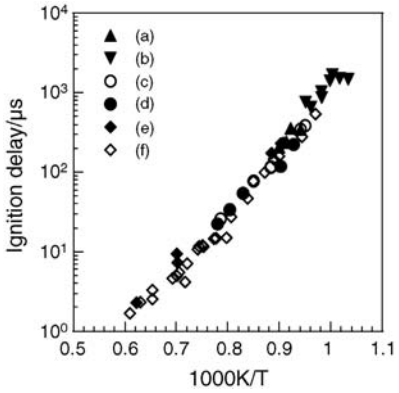

Figure 3.30 Ignition delay of kerosene–air mixtures; a: Jet A at 30 atm, b: JP-8 at 30 atm, c: Jet A at 20 atm, d: jet A at 10 atm, e: kerosene at 10 atm, f: Jet A at 10 atm. Reproduced with permission from [12].

3.4.11 Ignitability

Gasoline engines use induced ignition to bring about combustion; *spark plugs* (Figure 3.31) provide a "trigger" at the right point in time (time is measured in "degree crank angle" by automotive engineers). Essentially, a spark plug consists of two closely spaced electrodes between which a high voltage is applied so that a plasma is generated.

Each engine has a so-called "characteristic map", which defines the best ignition time based on load and engine speed. An example is given in Figure 3.32.

Conversely, Otto engines rely on auto-ignition of diesel injected into the engines' combustion chambers. Gasoline must not ignite too spontaneously, as this would

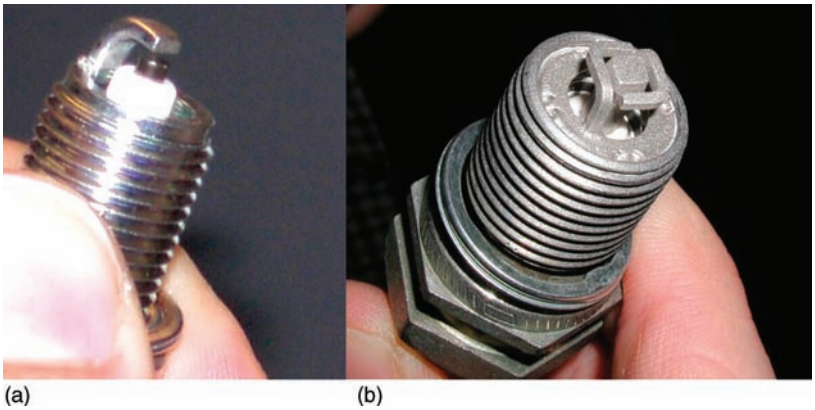

Figure 3.31 Spark plug for induced ignition in an automotive Otto engine (a) and a large, stationary gas engine (b).

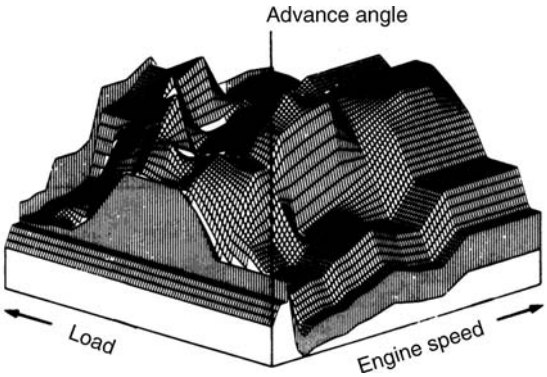

Figure 3.32 Characteristic map of an engine, showing the optimum ignition time. Source [13].

produce so-called "engine knock" which is accompanied by dangerous pressure spikes (see Figure 3.33). On the other hand, diesel has to be rather easy to ignite at the desired temperature and pressure. A measure of the "ignitability" of fuels is given by the octane number in the case of gasoline, the cetane number in the case of diesel and the methane number in the case of gaseous fuels.

Diesel engines, which are based on autoignition, use a glowplug (Figure 3.34). This is a small heating device which helps overcome excessive heat losses at engine start. Glow plugs reach temperatures of around 850 °C. Preheating takes 10 s or more for older engines and a few seconds only in newer ones.

3.4.12
Octane Number

The octane number (ON, octane rating) is a measure of the quality of automotive and aviation fuels. The lower the octane number, the more easily the fuel will autoignite.

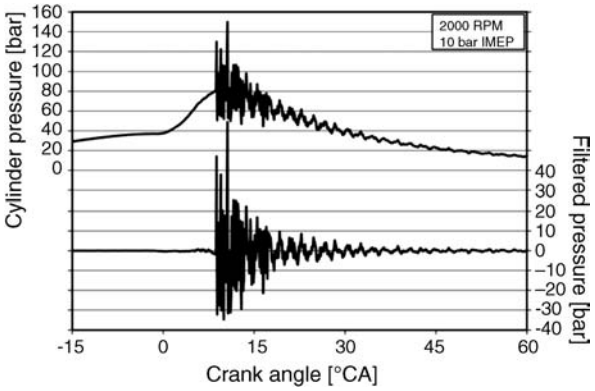

Figure 3.33 Typical cylinder pressure trace for heavy knocking in an engine. RPM = rotations per minute, IMEP = indicated mean effective pressure. Reproduced with permission from [14].

Figure 3.34 Glow plug for diesel engines. Reproduced from [15].

ON can be measured in a test engine and is defined by comparing a given fuel with the mixture of 2,2,4-trimethylpentane (iso-octane) and n-heptane with the same knocking properties as the fuel under investigation. Pure iso-octane is set at 100 (low knocking propensity) and heptane at 0 (high knocking properties). The selection of n-heptane as the zero point of the scale was made because of its availability in high purity at the time of introduction. "*Knocking*" is an undesired, fast combustion process characterized by high pressure spikes to due sudden autoignition of fuel/air in Otto engine cylinders. It can destroy an engine.

Avgas (aviation gasoline) is comparable to automotive gasoline (mogas, motor gasoline) except that it is used as aviation fuel for piston-engine aircraft. Avgas still contains tetraethyl lead (TEL) as anti-knock agent. For mogas, MTBE (methyl *tert*butyl ether) is used to enhance combustion stability.

Depending on the test method, one can distinguish between RON and MON (RON = research octane number, MON = motor octane number). Otto engines generally tolerate fuel with a higher-than-specified octane number.

3.4.13
Cetane Number

The cetane number (CN, cetane rating) is a measure of a diesel fuel combustion performance, more specifically the fuel's ignition delay. Higher cetane fuels have shorter ignition delay times. Generally, diesel engines use fuels with CN between 40 and 55. Biodiesel has a typical CN of 46 to 52.

Cetane is a mix of unbranched, aliphatic alkane molecules. It ignites very easily under compression, so it was assigned a cetane number of 100, whereas alpha-methylnaphthalene was given a cetane number of 0. Real diesel fuels are indexed to cetane as to how well they ignite under compression. The cetane number therefore measures how quickly the fuel starts to burn (autoignites) under diesel engine

conditions. Other quality parameters of diesel fuel are its density, lubricity, cold-flow properties and sulfur content.

Comment: For gaseous fuels, an important quality parameter is the methane number.

3.4.14
Ignition in Various Combustion Devices

Power plants are started with pilot burners. Gasoline engines use electric spark plugs (see above). Although spark plugs have been in use for more than a century, they have inherent disadvantages so that researchers have been looking for alternative modes of induced ignition.

An alternative ignition system is laser-induced ignition (*laser ignition*) [16,17] (see Figure 3.35).

An obvious advantage of optical ignition is the free choice of the ignition location. Conventional spark plugs can only ignite the fuel/air mixture at the vessel wall, because otherwise the protruding metal would disturb the fluid flow. Due to system costs and difficulties with a suitable window material, no commercial laser ignition system has made it into automotive cars yet. However, several missiles are fired using laser ignition.

Other alternative ignition systems for automotive engines are (see Figure 3.36)

- High frequency ignition [19]
- Microwave ignition [18,20]
- Corona ignition [18]
- Plasma-assisted ignition [21,22,18]

Two further ignition concepts for automotive engines are "*skip cycle ignition*" [23] and HCCI (*homogeneous charge compression ignition*) [24]. In R&D, *shock tube ignition* [25] is also utilized. See [26] for a summary on alternative ignition systems.

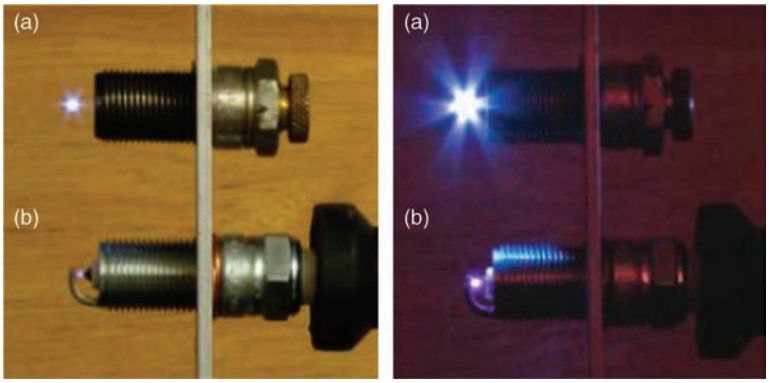

Figure 3.35 Comparison of (a) an optical spark plug (laser ignition) and (b) conventional, electrical spark plug. Reproduced with permission from [17].

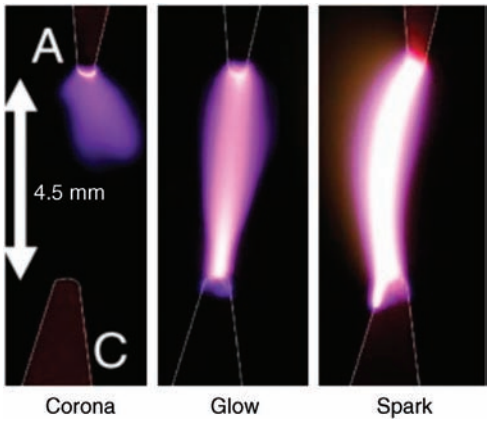

Figure 3.36 Appearance of corona, glow and spark discharges. Reproduced from [18].

3.4.15 Undesired Ignition

For safety reasons, undesired ignition and, worse, undesired explosion, of combustible materials has to be avoided. Basically, not only fuels, but all combustible materials are at risk for undesired ignition. The larger the stored volume, the higher the risk for damage and loss in the case of a fire will be. Figure 3.37 shows an example of an undesired ignition with huge consequences: the Buncefield fire in a UK oil storage terminal in December 2005.

Safety starts with proper process design [3]. The flammability is a critical property for building materials, as specified by DIN 4102 and EN 13501. A classic textbook on ignition in this context is [28]. See also [29,30] and Chapter 7 in this book.

Figure 3.37 Buncefield site prior to incident and showing the major fires that followed the explosion. Reproduced with permission from [27].

References

1 Knothe, G., Matheaus, A.C., and Ryan III, T.W. (2003) Cetane numbers of branched and straight-chain fatty esters determined in an ignition quality tester. *Fuel*, **82** (8), 971–975.

2 Babrauskas, V. (2003) *Ignition Handbook: Principles and Applications to Fire Safety Engineering, Fire Investigation, Risk Management and Forensic Science*, Fire Science Publications, ISBN: 978-0972811132.

3 Kjellén, U. (2007) Safety in the design of offshore platforms: Integrated safety versus safety as an add-on characteristic. *Safety Science*, **45** (1–2), 107–127.

4 Reed, J.R. (1986) *North American Combustion Handbook*, 3rd edn, vol. 1, North American Manufacturing Corporation, Cleveland, OH, USA.

5 Bouali, Z., Pera, C., and Reveillon, J. (2012) Numerical analysis of the influence of two-phase flow mass and heat transfer on n-heptane autoignition. *Combustion and Flame*, **159** (6), 2056–2068.

6 Warnatz, J., Maas, U., and Dibble, R.W. (2006) *Combustion: Physical and Chemical Fundamentals, Modeling and Simulation, Experiments, Pollutant Formation*, 4th edn, Springer, ISBN: 978-3540259923.

7 Meyer, R. (1987) *Explosives*, 3rd edn, Wiley-VCH Verlag GmbH, ISBN: 978-3527265992.

8 White, C.M., Steeper, R.R., and Lutz, A.E. (2006) The hydrogen-fueled internal combustion engine: a technical review. *International Journal of Hydrogen Energy*, **31**, 1292–1305.

9 Davy, H. (1817) Some new experiments and observations on the combustion of gaseous mixtures, with an account of a method of preserving a continued light in mixtures of inflammable gases and air without flame. *Philosophical Transactions of the Royal Society of London*, **107**, 77–85, http://www.jstor.org/stable/107574 (accessed June 1, 2013).

10 Bonner, B.H. and Tipper, C.F.H. (1965) The cool flame combustion of hydrocarbons I—Cyclohexane. *Combustion and Flame*, **9** (3), 317–327.

11 Pearlman, H. (2007) Multiple cool flames in static, unstirred reactors under reduced-gravity and terrestrial conditions. *Combustion and Flame*, **148** (4), 280–284.

12 Dagaut, P. and Cathonnet, M. (2006) The ignition, oxidation, and combustion of kerosene: A review of experimental and kinetic modeling. *Progress in Energy and Combustion Science*, **32** (1), 48–92.

13 Sachenbacher, M. and Williams, B.C. (2005) *Automated Model Generation Using Qualitative Abstraction*, CSAIL, MIT Computer Science and Artificial Intelligence, Laboratory, http://publications.csail.mit.edu/abstracts/abstracts05/mers2/mers2.html#fig1 (accessed June 1, 2013).

14 Verhelst, S. and Wallner, T. (2009) Hydrogen-fueled internal combustion engines. *Progress in Energy and Combustion Science*, **35** (6), 490–527.

15 http://www.turbocompressori.net/glow_plugs.htm (2012) (accessed 1 June 2013).

16 Puhl, M. (2011) *Corona and Laser Ignition in Internal Combustion Engines: A Comparison to Conventional Spark Plug Ignition*, VDM Verlag Dr. Müller, ISBN: 978-3639323115.

17 Morsy, M.H. (2012) Review and recent developments of laser ignition for internal combustion engines applications. *Renewable and Sustainable Energy Reviews*, **16** (7), 4849–4875.

18 Starikovskiy, A. and Aleksandrov, N. (2013) Plasma-assisted ignition and combustion. *Progress in Energy and Combustion Science*, **39** (1), 61–110.

19 Bae, C., Lee, J., and Ha, J. (1998) High-Frequency Ignition Characteristics in a 4-Valve SI Engine with Tumble-Swirl Flows, SAE Technical Paper 981433. doi: 10.4271/981433.

20 Meir, Y. and Jerby, E. (2012) Thermite powder ignition by localized microwaves. *Combustion and Flame*, **159** (7), 2474–2479.

21 Starikovskiy, A. and Aleksandrov, N. (2013) Plasma-assisted ignition and combustion. *Progress in Energy and Combustion Science*, **39** (1), 61–110.

22 Starikovskii, A.Yu. (2005) Plasma supported combustion. *Proceedings of the Combustion Institute*, **30** (2), 2405–2417.

23 Kutlar, O.A., Arslan, H., and Calik, A.T. (2007) Skip cycle system for spark ignition engines: An experimental investigation of a new type working strategy. *Energy Conversion and Management*, **48** (2), 370–379.

24 Zhao, F. (2003) *Homogeneous Charge Compression Ignition (HCCI) Engines: Key Research and Development Issues*, Society of Automotive Engineers, ISBN: 978-0768011234.

25 Vasu, S.S., Davidson, D.F., and Hanson, R. K. (2008) Jet fuel ignition delay times: Shock tube experiments over wide conditions and surrogate model predictions. *Combustion and Flame*, **152** (1–2), 125–143.

26 Lackner, M. (ed.) (2009) *Alternative Ignition Systems*, ProcessEng Engineering GmbH, Wien, ISBN: 978-3-902655-05-9.

27 Michael Johnson, D. (2010) The potential for vapour cloud explosions – Lessons from the Buncefield accident. *Journal of Loss Prevention in the Process Industries*, **23** (6), 921–927.

28 Lewis, B. and Von Elbe, G. (1987) *Combustion, Flames & Explosions of Gases*, 3rd edn, Academic Press Inc., ISBN: 978-0124467514.

29 Hattwig, M. and Steen, H. (2004) *Handbook of Explosion Prevention and Protection. An Evidence-Based Review*, 1st edn, Wiley-VCH, ISBN: 978-3527307180.

30 Lackner, M. Winter, F. and Agarwal, A.K. (eds) (2010) *Handbook of Combustion*, Wiley-VCH Verlag GmbH, ISBN: 978-3527324491.